

Dear Editor,

Thank you for taking your time to handle and report on our manuscript. Hereby, we would like to provide our point-by-point reply to the comments of Anonymous Referee #1 (AR#1) and Anonymous Referee #2 (AR#2). Finally, we also respond to the remark from the editor.

Original comments are marked by the referee abbreviation 'AR#1' or 'AR#2', the remark by the editor by 'Editor', our responses by 'Authors' and reference to the places where changes have been made in the track-changes version of the manuscript are marked by 'Change'. In addition to the changes following the comments by AR#1, AR#2 and Editor, we have made minor text editions to correct spelling/grammar or increase readability. All text changes are visible in the track-changes version of the manuscript. Note that the track-changes file does not mark changes for remade figures. The figures that have been remade are Fig. 3, 5, 6, 8, A1, A4, A5, A6 and A7.

Response to comments by Anonymous Referee #1

- | | | |
|-----|---------|------------------------------------------------------------------------------------------------------------------------------------------------------------------------------------------------------------------------------------------------------------------------------------------------------------------------------------------------------------------------------------------------------------------------------------------------------------------------------------------------------------------------------------------------------------------------------------------------------------------------------------------------------------------------------------------------------------------------------------------------------------------------------------------------------------------------------------------------------------------------------------------------------------------------------------------------------------------------------------------------------------------------------------------------------------------------------------------------------------------------------------------------------------------------|
| 1.1 | AR#1 | The paper has a very clear structure and additional division of the assessment into different scales, making it clear which data and methods are used for which scale and analysis. The combination of datasets (including not only meteorological but also hydrological ones) on various scales gives the chance to assess the drought situation of 2018 for this region in more detail. The results of the analysis are explained and discussed in detail (which is good in general) but can lead to difficulties to follow all the information presented and taking away the key findings. Adding a small subchapter at the end of Section 5 with parts of the conclusion, where all the results are placed together, would help to connect the different discussion parts already earlier and leave more space for an even more concise conclusion. The figures used are nicely selected and interesting, especially Fig.8 including the groundwater response to precipitation and Fig.1 and 2 to highlight the streamflow and groundwater regimes, allowing the reader to get a better understanding of the hydroclimatological characteristics of the case area. |
| | Authors | The structure of the discussion chapter was something we discussed extensively during the writing process, in particular the discussion related to drought propagation. Currently the discussion regarding 2018 drought propagation is embedded in Sect. 5.2. Following the suggestion, we considered adding a new subsection at the end of Section 5 bringing together the key results in the context of drought propagation by moving parts of the content from the conclusion and Sect. 5.2. However, we find the original structure of the discussion the better option, in which the drought propagation becomes a natural part of the discussion of the hydrological aspect of the drought. |
| | Change | No change in manuscript. |
| 1.2 | AR#1 | The introduction is giving an overview of the general drought situation and impacts for this region, elaborating on the study area and setting the stage for the study by recapping the general definition of drought, drought studies and their difficulties in regards to appropriate data selection and use. Further, a section on the large scale atmospheric drivers is giving, which is part of the later assessment. An additional elaboration on the other methods included and the reasoning behind using them would help prepare the reader for the following analysis and results and would strengthen the introduction and emphasising why this paper is special in its own way and closing current |

		research gaps. Adding more information on this and mentioning more similar studies might also help setting the scene for a deeper discussion later on.
Authors		We agree on including a more complete presentation of the methods applied, including their motivation as well as potential similar studies not already mentioned in the introduction. We have embedded this in our revised version.
Change		Page 4: line 21-34.
1.3	AR#1	The analysis is focused on the extremeness of the months May-August 2018, as mentioned in the abstract and introduction, highlighting the situation on conditions for northern European countries in that period. Despite stating the aim of the study clearly in the introduction, the title can lead to a slight misunderstanding. Nevertheless, having done such an extensive analysis of various aspects of the hydrological cycle for the whole year (as given by the information in the supplement), I personally think including some more lines on the results and observation in early spring until the end of the year, besides the extreme events observation in the period of May-August 2018, would create an even better base to start a wholesome discussion. Especially, as the findings are currently discussed within the light of the whole annual cycle (Sec.5.2) and it is mentioned that antecedent water storage (initial conditions) play an important role in the occurrence, timing and development of hydrological droughts and drought propagation. Extending the results and discussion to months where drought characteristics were also observed in April and autumn months (e.g. Fig A6 (SPI3), A7 (SPEI3), A9 and Fig.8 (groundwater ranks and groundwater response to precipitation)), could help to create an even better understanding of the drought situation of 2018. This in the end might help to create an even stronger discussion and to put the work into more context by being able to connect it to other drought studies of 2018 throughout Europe, bringing together other strains of research and closing the picture of the drought 2018.
Authors		We agree that it is a good idea to include some more lines about the early spring until the end of the year, and we have done this in our revised version. We find your comment to extend the discussion beyond May-August 2018, valuable in that potential future studies on the 2018 drought can more easily connect it to our paper if accepted.
Change		Page 11: line 10-11, 22-23, 29-31. Page 12: line 25-27, 34-35. Page 13: line 1-2, 5-7, 12-19, 30-31. Page 16: line 27. Page 17: line 30-31. Page 18: line 19-22, 35. Page 19: line 1-2.
1.4	AR#1	Table 1: adding an additional column for the observed impact category (e.g. agriculture, energy sector, etc.) would make table even more complete and could reduce effort to write all examples out in text
Authors		We agree it is a good idea to include the impact category in Table 1, and we have done so in our revised version following the EDII categorisation provided in Stahl et al. (2016; doi:10.5194/nhess-16-801-2016). We also changed parts of the set-up of the table (mainly the order of the columns) to make it more easily readable. In the discussion format of the paper, the table is larger than one page, however, in the two-column format, it fits nicely into one page (see snap shot at the end of this document). If the former is a problem, we can optionally move the URLs to another location, e.g. by making a list of URLs after the reference list. We could not find any house rules related to handling URLs, so if we are to change the format of the table and potentially move the URLs, specific guidelines on how this is preferably done, are appreciated.
Change		Table 1 on page 27.

- 1.5 AR#1 p5 line21: 3 stations within mountain regimes mentioned which were highly influenced by glaciers, were they treated differently in the analysis or just included in the average?
- Authors We are not sure which average is referred to here, but the regimes highly influenced by glaciers were not treated differently from the other regimes in the analysis. Accordingly, the stations are included in the total percentages of stations affected and in the EOF analysis in the same way as the other stations (also reflecting widely different regimes).
- Change No change in manuscript.
- 1.6 AR#1 p5 line34: has instead of have (twice)
- Authors This has been corrected.
- Change Page 6: line 25.
- 1.7 AR#1 Data and methods section in general: focus on historical analysis: In regards to human influence there was a careful selection of near natural groundwater wells but to what extent was climate change reconsidered in the analysis and the trend that might have been included automatically in the datasets used?
- Authors Climate change was not considered explicitly in the analysis of the 2018 drought, and accordingly, potential trends in both the average and extreme conditions are automatically included. The main purpose of the ranking maps was to investigate the extremeness of individual months in 2018 as compared to the historical record. On the other hand, the purpose of the EOF analysis was to detect main patterns in summer streamflow variability, and linear detrending of the JJA streamflow time series was conducted prior to the EOF calculation (ref. p9, line 27-28).
- Change No change in manuscript.
- 1.8 AR#1 Results and discussion section in general: also include beginning and end of the year results next to extremeness of summer months if mentioned later on in discussion (for example HGT500 from April might already indicate how situation in May could look like)
- Authors We agree, and interpret this comment as being related to comment 1.3 and 1.15.
- Change See reply to 1.3 and 1.15
- 1.9 AR#1 Fig. 4 and Fig. A3 using the same range for HGT500 values for all months presented would allow to compare values between months more easily. Additional question to Fig.4: why aggregate over May-August (as most other results presented are shown separately per month)?
- Authors We did not seek to have the same scale on the HGT500 axes; rather focus on depicting the relative variability for each month using standard deviation (thus allowing direct comparison of the variability as such). We made a figure for our online response to AR#1 showing the same figure as Fig. A3 in the paper, except that the same range is used for HGT500 values in the right panel. Accordingly, the time series shifts its location (up or down) along the HGT500 axis. We do not see any advantage of presenting the results in this way, and prefer to keep the figure as it is. Nevertheless, we will add a remark that the range is different, to ease the interpretation for the reader. Figure 4 is provided to emphasise the extreme overall large-scale atmospheric situation in the

		<p>period May-August. Combined with separate monthly plots in the Appendix (Fig. A3), we think this provides an informative overview for the reader.</p> <p>Change Page 41, added sentence in the Fig. A3 caption: <i>“Note the different ranges of the y-axes.”</i></p>
1.10	AR#1	<p>General comment on ranking system: nice to highlight extremes (as it is one of the goals mentioned in the introduction) but additional information and figures on mean historical temp vs 2018 temp would help to put this into place in regards to absolute values, also helps to understand precipitation observations as not that many low extremes were recognised but in SPI3 drought is indicated</p> <p>Authors We agree that this is interesting additional information. We have made anomaly maps for each month in 2018 of temperature and precipitation and added these to the supplement.</p> <p>Change Supplement Figure S1 and S2. Referred to in the main text on: Page 12: line 10, 29. Page 18: line 12, 20.</p>
1.11	AR#1	<p>Fig10: what was the reasoning to switch to months June-August for this analysis, compared to the other results that have been heavily focused on period May-August?</p> <p>Authors The main reason to use June-August instead of May-August in the composite maps (Fig. 10), was to use the same period as used for the EOF analysis of streamflow that the composites are based on. The main reason for using June-August instead of May-August in the EOF analysis was to avoid the effect of high flow in May caused by snowmelt. Furthermore, EOF analysis and composite maps are traditionally done on a three-month seasonal basis, making the results more easily comparable to other studies. We have made the reasoning behind the choice of June-August more clear in the text in our revised version.</p> <p>Change Page 10: line 31-33. Page 11: line 1. We have added two sentences: <i>“The June-August period was chosen for the EOF analysis (rather than May-August, which is in focus in Sect. 3.1-3.3) to avoid the effect of high flow in May caused by snowmelt. Furthermore, EOF analysis and composite maps are traditionally done on a three-month seasonal basis, making the results more easily comparable to other studies.”</i></p>
1.12	AR#1	<p>Discussion, section about annual hydrological cycle: more information and figures about initial conditions (e.g. snowfall) in supplement (e.g. annual averaged timeseries and 2018 situation, similar to Fig.1 and 2) and citations would support and help to follow the explanation of the specific observations and putting them into more context (some good starting information was already given in introduction about the hydroclimatological characteristics, streamflow and groundwater regimes)</p> <p>Authors Observed annual average time series plotted along with the 2018 time series for each streamflow and groundwater station, were made as part of the initial analysis, but not included in the paper itself due to the article already being relatively long. We agree that they can help support the interpretation and discussion. We have now made figures of standardised monthly average streamflow and groundwater levels in 2018 vs multiyear monthly statistics for each station separately, and added them to the supplement. We will not include data of initial conditions, such as snow and soil moisture for each catchment, as this would require using modelled data.</p>

- Change Supplement Figure S3—S5 (streamflow) and Figure S6—7 (groundwater). Referred to in the main text on: Page 6: line 11. Page 7: line 3. Page 13: line 27, 33. Page 14: line 1. Page 17: line 23, 28. Page 18, line 15, 31.
- 1.13 AR#1 p16 line2: citations or other examples to underline this assumption?
 Authors We removed the part of the sentence where we speculate about the role of persistent groundwater contribution, to connect the sentence directly to the argument of the previous sentence.
 Change The text now reads (page 18: line 4-8): *“A southeastern-northwestern gradient in extreme temperature (and SPEI3) this month, however, reflects the spatial pattern of extremely low streamflow in Denmark, indicating that higher than usual evapotranspiration rates likely contributed to extreme conditions in the southeast. Correspondingly, less extreme evapotranspiration in the west and north might have prevented streamflow drought to develop there.”*
- 1.14 AR#1 p16 line14-16: could you elaborate a bit more (e.g. references to figures where this is observed). If I look at Fig A9, A8, A7 for example I see overlapping areas and stations with indicate drought occurrence?
 Authors We agree that there are overlapping areas and stations which indicate drought occurrence. Our point about the high local variability was that several wells have no rank 1-6 at locations where other wells have rank 1-6. We have clarified what we mean in the text.
 Change The sentence now reads (page 18: line 26-28): *“The high spatial variability in hydrogeological properties across the Nordic region is mirrored in the diversity in groundwater response to meteorological conditions, as reflected in a high local variability for groundwater drought (rank between 1 and 6) even for closely located wells.”*
- 1.15 AR#1 p16 line24: would you say this is already the effect of drought propagation one can observe (with the ongoing dry conditions until the end of the year (e.g. seen in SPEI3 results)?
 Authors We interpret your question as to whether the below normal groundwater levels at end 2018 /start 2019 are a response to the summer 2018 event or caused by dry conditions following the below normal rainfall September-November 2018. It is probably a combined effect of the two. Following the inclusion of the situation in the spring and autumn (ref. third comment), we will embed an assessment of both the streamflow and groundwater conditions related in the revised version.
 Change Page 18: line 19-22, 35. Page 19: 1-2.
- 1.16 AR#1 p17 line8-9: maybe include this reference already in introduction to set the stage for the discussion
 Authors We were unable to find a natural place for these references in the introduction without adding a new paragraph related to assessments of historical drought events in Europe. We prefer to not increase the size of the (in our opinion) already long introduction in order to include these references there.
 Change No change in manuscript.
- 1.17 AR#1 p 17 line25, spelling error: wells instead of well.
 Author This has been corrected.
 Change Page 20: line 9.

- 1.18 AR#1 Appendix: A1 mountain regime: why not include December as winter month for classification criteria for streamflow regime?
 Authors The reason is that none of the stations have minimum or a second minimum flow in December (the same is true for November). We will add a note about this in Appendix A1. November/December is typically the beginning of the winter season, and lowest flow for stations with winter low flow regime typically occurs towards the end of the winter season (most winter low flow regime stations have minimum flow in February and March).
 Change Page 37: line 13-14. Added the sentence: *“November and December were not included in the low flow season because none of the streamflow stations had the minimum or second minimum flow in these months.”*
- 1.19 AR#1 A1 line7: missing point after class
 Authors This has been corrected.
 Change Page 37: line 7.

Response to comments by Anonymous Referee #2

- 2.1 AR#2 P4L24: Do the temperature data here refer to 2 m temperature?
 Authors The E-OBS temperature data is interpolated station data of air temperature. We asked this question to the E-OBS project team. They answered that temperature is not always measured at 2 meters by all data providers, they do not know the exact measuring height for all data providers, and they do not correct measurements to have a ‘standard’ height.
 Change No change in manuscript.
- 2.2 AR#2 P4L31-32: I am wondering why do the authors use 2 different spatial scales for analyses in section 3.1 and 3.2 (0.25°), and 3.3 (0.1°)? Why do not simply use a spatial resolution of 0.1°?
 Authors We agree that this is confusing, and in the revised version of the manuscript we use the resolution of 0.1 for all analysis and figures using the E-OBS dataset. Since the E-OBS dataset has been updated after we made the figures used in the original manuscript, we have used the newest available version (v21.0e) when remaking the figures. The percentages of grid cells with SPI3 and SPEI3 <- 1.5 are updated according to the new dataset.
 Change Figure 5 (page 31), 6 (page 32), 8 (page 34), A4 (page 42), A5 (page 43), A6 (page 44) and A7 (page 45) are remade, and Figure S1 and S2 in the supplement are made, using the E-OBS dataset v21.0e at 0.1deg resolution. Data description changed on page 5: line 16-18. Percentages changed on page 13: line 8, 21-22.
- 2.3 AR#2 P8L15: The authors may write: three-month.
 Authors This has been corrected.
 Change Page 9: line 13, 25. Page 28: two times in Table 2.
- 2.4 AR#2 P8L27-29: Here, I am also wondering why do the authors use SPI-3 (SPEI-3) distributions derived from the data year 1971 to 2000 to calculate SPI-3 (SPEI-3) in the year 2018? Why do not use the distribution derived from 1971 to present data? By only using data from 1971 to 2000 (20 years ago), the drought 2018 might be too extreme because the authors excluded extreme drought years e.g. 2003, 2006-2008, and 2015. This has implications in the distributions that the authors used. Moreover, the average temperature >20 years ago was lower

		<p>than the average temperature in the past 20 years (2000-2020). In Europe, we also use drought years 1976 and 2003 as a benchmark for extreme drought years. 2018 was comparable to those years in terms of drought severity. This question applies to other reference data (e.g. section 3.1, from 1981 to 2000).</p>
Authors		<p>We agree that the extremeness of the anomaly plots as well as SPI3 and SPEI3 can be sensitive to the choice of reference period. The reason we use a 30-year period of reference (ref. WMO guidelines) and not the period 1971 to 2018 is to allow for easier comparison with other studies (e.g. Ionita et al., 2017; doi:10.5194/hess-21-1397-2017). Even though a 30-year period of reference might be subject to choice, it is more consistent than using a longer period up to the year of interest. A key focus of our study was to use the ranking maps to investigate the historical extremeness compared to other extreme years during the whole 60-year period. The main purpose of including the SPI and SPEI figures was to map the dynamic (in space and time) of the meteorological drought. Following the reviewer's remark, we calculated the SPI and SPEI using the whole period (1959-2018) as reference (figures in our online response to AR#2), and found similar spatial patterns in the drought evolution throughout 2018 (ref. monthly plots). Accordingly, we prefer to keep the 30-year period of reference (i.e. 1971-2000).</p>
		<p>The SST reference period (originally 1981-2000) was the closest we could get 1971 to 2000 due to shortage of data. However, we agree that it is beneficial to use the same period of reference for all analysis. We have chosen to use the monthly SST data from the Hadley Centre (HadISST) for the SST anomaly calculations. The HadISST dataset has a coarser spatial resolution, but we were able to use the reference period 1971-2000. We have remade the SST figures using the HadISST data and 1971-2000 as reference period.</p>
Change		<p>Figure 3 (page 29) and Figure A1 (page 39) are remade using the HadISST dataset and the ref. period 1971-2000. Reference period changed on page 7: line 2, page 11: line 9, page 28 (in Table 2), page 29 (in figure caption), page 39 (in figure caption). Results changed on page 1: line 7, page 11: line 16. Data description changed on page 5: line 12-14, page 22: line 1-2.</p>
2.5	AR#2	<p>P9L4-6: I am wondering why do the authors use absolute values to determine the SPI classes? Figure 6 also shows the SPI/SPEI index values from -3 to +3.</p>
	Authors	<p>If we understand your comment correctly, the confusion may arise from displaying absolute values rather than the wet and dry ranges. We separate between negative and positive values in the study, and have clarified this in the revised version.</p>
	Change	<p>Page 10: line 1-6.</p>
2.6	AR#2	<p>P10L3: The authors may write as Figure 3a-d.</p>
	Authors	<p>We have included this in the revised version.</p>
	Change	<p>Page 11: line 9</p>
2.7	AR#2	<p>P10L11: The authors may write as Figure 3e-h.</p>
	Authors	<p>We have included this in the revised version.</p>
	Change	<p>Page 11: line 19.</p>
2.8	AR#2	<p>P12L30: Please write the Figure number after the sentence thus the reader can follow the description easily. Here is Figure 9a.</p>

- Authors We have included the figure numbers in the revised version. We also added reference to Figure 9d, 9e and 9f where appropriate.
Change Page 14: line 24, 26, 29, 32.
- 2.9 AR#2 P12L33: The authors may write Figure 9b after the sentence.
Authors We have included this in the revised version.
Change Page 14: line 27.
- 2.10 AR#2 P13L2: The authors may write Figure 9c after the sentence.
Authors We have included this in the revised version.
Change Page 14: line 30.
- 2.11 AR#2 P14L20: Typo “than 3 std, respectively 2 std”
Authors We are not sure what typo it is referred to. We see that ‘std’ jumped to the next line, and have now forced it to be on the same line as the values.
Change Page 16: line 17.
- 2.12 AR#2 P24: Table 1: The author may write last accessed before the date. E.g. (last accessed 24.03.20).
Authors “URL (last access)” is written in the column heading to indicate that the date in parenthesis is the last access date. To make the table more clear, and adding impact category after comment 1.4, the structure of the table has been changed. We have also changed from “last access” to “last accessed”.
Change Table 1, page 27.
- 2.13 AR#2 P25: Back to my question about the reference data, here in Table 2, the authors indicate that they have temperature, precipitation, Geopotential height at 500MB data up to the year 2018.
Authors Yes, Table 2 shows the data used for the different indices. Currently the reference period 1971-2000 is kept (ref. answer to comment 2.4). We have updated the table following the change in reference period for the SST anomaly calculation (ref. answer to comment 2.4).
Change Period of reference for SST anomalies changed in Table 2 (page 28).

Editor’s remark

- 3.1 Editor Concerning the remark of one of the authors on other studies on the 2018 drought the following: our group also has a manuscript in discussion (<https://hess.copernicus.org/preprints/hess-2020-358/>, feel free to comment), and there will be a special issue in Phil. Trans. R. Soc. B, see: <https://royalsocietypublishing.org/rstb/forthcoming-issues>. If it comes out soon it might be useful to you in the revision.
- Authors We thank the editor for good suggestions of 2018 papers, related to comment 1.3. The first suggestion concerns an interesting study of the 2018 drought’s effects on root water uptake and a quantification of the critical moisture content in the Netherlands. We included this reference in the paragraph concerning energy-limited vs water-limited regions. The other suggestion is the now available special issue about the 2018 drought/heatwave impacts (<https://royalsocietypublishing.org/toc/rstb/375/1810>). Our impression is that the main focus is on the impact on terrestrial ecosystems (including crops). As

we already have examples of those impacts in the introduction, we choose to not include them in the revised version.

Change Page 17: line 3.

2 S. J. Bakke et al.: The 2018 northern European hydrological drought and its drivers in a historical perspective

Table 1. Reports and news articles about 2018 heat and drought related impacts. The impact categories follow the EDII Impact categorisation (Stahl et al., 2016).

Ref.	Impact category	Region	Publisher	URL (last updated/last accessed)
a	Wildfires	Europe	Joint Research Centre, European Commission	https://op.europa.eu/en/publication-detail/-/publication/435ef008-14db-11ea-8c1f-01aa75ed71a1/language-en (29.11.18/24.03.20)
b	Agriculture and livestock farming	European Union	Agriculture and Rural Development, European Commission	https://ec.europa.eu/info/news/drop-eu-cereal-harvest-due-summer-drought-2018-oct-03_en (31.10.19/24.03.20)
c	Agriculture and livestock farming	European Union	Reuters	www.reuters.com/article/us-europe-grains-analyst/analysts-cut-eu-wheat-crop-outlook-again-on-catastrophic-north-idUSKBN1KU15E (09.08.18/24.03.20)
d	Agriculture and livestock farming (mainly)	Europe	Euronews	www.euronews.com/2018/08/10/explained-europe-s-devastating-drought-and-the-countries-worst-hit (12.08.18/24.03.20)
e	Agriculture and livestock farming	Sweden	Swedish Board of Agriculture	https://www2.jordbruksverket.se/download/18.21625ee16a16bf0cc0eed70/1555396324560/ra19_13.pdf (16.04.19/24.03.20)
f	Agriculture and livestock farming	Norway	Norwegian Agriculture Agency	www.landbruksdirektoratet.no/no/statistikk/landbrukserstatning/klimarelaterte-skader-og-tap/avlingssvikt-statistikk (02.09.19/24.03.20)
g	Energy and industry	Norway, Sweden, Finland	Norwegian Water Resources and Energy Directorate	www.nve.no/Media/7385/q3_2018.pdf (17.10.18/24.03.20)
h	Energy and industry	Norway	newsinenglish.no	www.newsinenglish.no/2018/07/13/drought-blamed-for-high-electricity-rates/ (13.07.18/24.03.20)
i	Waterborne transportation	Germany	Handelsblatt Today	www.handelsblatt.com/today/companies/low-water-dwindling-rhine-paralyzes-shipping-transport/23695020.html?tickets=ST-3121873-yvfwqilee3yWiy3BK1Zv-ap4 (27.11.18/24.03.20)
j	Waterborne transportation	Hungary	Reuters	www.reuters.com/article/us-europe-weather-hungary-shipping/water-levels-in-danube-recede-to-record-lows-hindering-shipping-in-hungary-idUSKCN1L71DH (22.08.18/24.03.20)
k	-	Germany	Deutsche Welle	www.dw.com/en/hot-weather-exposes-world-war-ii-munitions-in-german-waters/a-44924959 (02.08.18/24.03.20)
l	-	Czech Republic	Business Insider	www.businessinsider.com/sinister-hunger-stones-dire-warnings-surfaced-europe-2018-8?r=US&IR=T (27.08.18/24.03.20)
m	Freshwater ecosystems	Norway	Adresseavisen	www.adressa.no/nyheter/trondelag/2018/07/28/Gaula-stengt-for-fiske-pa-grunn-av-varmen-17208221.ece (30.07.18/24.03.20)
n	Public water supply	Sweden	The Local Sweden	www.thelocal.se/20190425/sweden-may-be-heading-for-a-new-water-crisis (25.04.19/24.03.20)

in 2018 compared to the more southerly located extreme drought in 2003 (Buras et al., 2020). Already in June, the water volumes in Nordic hydropower reservoirs dropped well below normal, which together with high fuel prices caused the July–August power rates to be the highest in 20 years (Table 1.g,h). Record low river levels disrupted main inland waterways in central Europe, forcing transportation ships to reduce their loads by up to 85 % (Table 1.i,j). Low water levels in the river Elbe exposed World War 2 munitions (Table 1,k) and so-called hunger stones with centuries old low

water level marks along with dire warnings (Table 1,l). Extremely low streamflow and high river temperatures led to fishing bans in major salmon fishing rivers in Norway (Table 1,m). Low groundwater tables led Swedish municipalities to ban residents from using water from the municipal network for anything other than drinking (Table 1,n). The high costs and wide range of impacts associated with the 2018 drought, emphasise the need to improve the understanding of such extreme, high impact events affecting large regions

Table 1 in HESS two-column format.

The 2018 northern European hydrological drought and its drivers in a historical perspective

Sigrud J. Bakke¹, Monica Ionita², and Lena M. Tallaksen¹

¹Department of Geosciences, University of Oslo, Oslo, Norway

²Alfred Wegener Institute Helmholtz Centre for Polar and Marine Research, Bremerhaven, Germany

Correspondence: Sigrud J. Bakke (s.j.bakke@geo.uio.no)

Abstract. In 2018, large parts of northern Europe were affected by an extreme drought. A better understanding of the characteristics and the large-scale atmospheric circulation driving such events is of high importance to enhance drought forecasting and mitigation. This paper examines the historical extremeness of the May–August 2018 meteorological situation and the accompanying meteorological and hydrological (streamflow and groundwater) drought. Further, it investigates the relationship between the large-scale atmospheric circulation and summer streamflow in the Nordic region. In May and July 2018, record-breaking temperatures were observed in large parts of northern Europe associated with blocking systems centred over Fennoscandia and sea surface temperature anomalies of more than 3 °C in the Baltic Sea (May, July) and the Barents Sea (July). Extreme meteorological drought, as indicated by the three-month standard precipitation index (SPI3) and precipitation-evapotranspiration index (SPEI3), was observed in May and covered large parts of northern Europe by July. Streamflow drought in the Nordic region started to develop in June, and in July 68 % of the stations had record-low or near-record-low streamflow. Extreme streamflow conditions persisted in the southeastern part of the region throughout 2018. Many groundwater wells had record-low or near-record-low levels in July and August. However, extremeness in groundwater levels and (to a lesser degree) streamflow showed a diverse spatial pattern. This points to the role of local terrestrial processes in controlling the hydrological response to meteorological conditions, including aquifer properties. Composite analysis of low summer streamflow and 500 mb geopotential height anomalies revealed a distinction between two distinct patterns of summer streamflow variability; one in western/northern Norway and one in the rest of the region. Low summer streamflow in western/northern Norway is was related to high-pressure systems centred over the Norwegian Sea. In the rest of the Nordic region, low summer streamflow is was associated with a high-pressure system over the North Sea and a low-pressure system over Greenland and Russia at similar latitudes, resembling the pattern of 2018. This study provides new insight into different hydro-meteorological aspects of the 2018 northern European drought, as well as identification of and identifies large-scale atmospheric circulation patterns associated with summer streamflow drought in the Nordic region.

1 Introduction

From May and throughout the summer of 2018, the northern and parts of central Europe experienced drought and record-breaking and persistent high temperatures leading to a variety of severe impacts, leading to severe impacts across a range of

sectors (Table 1). Drought is a complex phenomenon characterised by below average natural water availability ~~-,and-unlike~~ affecting all components of the hydrological cycle. Unlike most other natural hazards, it is a "creeping phenomenon" with a wide range of economic, societal, and environmental impacts gradually accumulating over time and space (Stahl et al., 2016; Mishra and Singh, 2010; Tallaksen and Van Lanen, 2004).

5 In 2018, wild fires destroyed vast areas in northern and central Europe. Sweden was especially impacted, with ~~record~~ breaking-record-breaking 24,310 ha (835 % of average) of burnt area (Table 1,a). The drought also led to significant drop in EU cereal production, whereas beef production grew more than expected due to increased slaughter following fodder shortage (Table 1,b). In Scandinavia and Germany, wheat and barley yields were described as catastrophically low (Table 1,c–f). Ecosystems in northern Europe are less adapted to extremely dry conditions ~~than~~ as compared to other European regions, and
10 direct negative impacts on terrestrial ecosystems productivity were both significantly stronger and ~~and~~-more widespread in 2018 compared to the more southerly ~~centred-located~~ extreme drought in 2003 (Buras et al., 2020). Already in June, the water volumes in Nordic ~~reservoirs for hydropower~~ hydropower reservoirs dropped well below normal, ~~and~~ which together with high fuel prices ~~it~~-caused the July–August power rates to be the highest in 20 years (Table 1,g,h). Record low river levels disrupted main inland waterways in central Europe, forcing transportation ships to reduce their loads by up to 85 % (Table 1,i,j). Low
15 water levels in the river Elbe exposed World War 2 munitions (Table 1,k) and so-called hunger stones with centuries old low water level marks along with dire warnings (Table 1,l). Extremely low streamflow and high river temperatures led to fishing bans in major salmon fishing rivers in Norway (Table 1,m). Low groundwater tables led Swedish municipalities to ban residents from using water from the municipal network for anything other than drinking (Table 1,n). The high costs and wide range of impacts associated with the 2018 drought, emphasise the need to improve the understanding of such extreme, high impact
20 events affecting large regions in Europe. The latter requires transnational data and international collaboration for ~~an~~-in-depth analysisanalyses.

To understand how the severity and timing of impacts vary among and within drought affected areas, it is important to distinguish between different stages of drought development. Typically, three types of drought are distinguished, reflecting the propagation of drought through the hydrological cycle; meteorological, soil moisture and hydrological (streamflow and
25 groundwater) drought (Tallaksen and Van Lanen, 2004). Meteorological drought refers to a precipitation deficit often combined with abnormal high (potential) evapotranspiration. If a meteorological drought is sustained, it typically causes soil moisture drought, which mainly ~~concern soil moisture~~ concerns water deficits in the root zone impacting water uptake by vegetation (Van Loon, 2015). When soil moisture depletes, a positive feedback loop ~~might~~ may occur due to ~~reduced~~ a reduction in the latent heat flux ~~-,making more energy available for~~ (less energy is used for evapotranspiration) and an associated increase in
30 the sensible heat flux (more energy is used to heat the air), which in turn increases the near-surface temperature (Seneviratne et al., 2010). Soil moisture drought can further reduce groundwater recharge and water sources that feed streams and rivers. This may, depending on the catchment characteristics and initial hydrological conditions, lead to groundwater and streamflow drought (Tallaksen and Van Lanen, 2004). Several studies have demonstrated how meteorological and hydrological droughts develop differently in space and time (e.g. Barker et al., 2016; Kumar et al., 2016; Haslinger et al., 2014; Vidal et al., 2010;
35 Tallaksen et al., 2009; Peters et al., 2003; Changnon, 1987). The delay between a meteorological and a hydrological drought

may amount to several months, with groundwater typically being the last to react and the last to recover (Hisdal and Tallaksen, 2000). The concept *drought*, ~~when used without specification unless specified~~, refers broadly to the multifaceted phenomenon that includes all three types of drought, along with their ~~different development and nature~~specific characteristics.

Many large-scale studies on drought focus on the meteorological aspect, such as anomalies in precipitation or climatic water balance (i.e. precipitation minus potential evapotranspiration), as this is based on data often easily at hand (e.g. Ionita et al., 2017; Stagge et al., 2017; Vicente-Serrano et al., 2014; Bordi et al., 2009). As opposed to meteorological data, transboundary near-real-time observations of hydrological variables ~~is~~are generally lacking, making timely observation-based, large-scale soil moisture, streamflow or groundwater drought assessments challenging (Liu et al., 2018; Laaha et al., 2016; Hannah et al., 2011). Long-term observational soil moisture data is sparse except for satellite based estimates ~~that only cover~~covering only a few centimetres depth (Hirschi et al., 2014; Kerr, 2007), which is too shallow to include the root zones of main vegetation types (e.g. Yang et al., 2016; Schenk and Jackson, 2002). ~~Data of updated~~Updated streamflow and groundwater level ~~usually needs~~observations usually need to be collected in a country-by-country based manner, which is time-consuming as well as challenging due to differences in agency structure, data quality requirements, availability of physiographic properties and information ~~of on~~ human influence. Despite these challenges, research on large-scale droughts cannot rely solely on meteorological data (Van Lanen et al., 2016). Drought assessments using hydrological data are needed to investigate the drought footprint on water resources, which is of high importance for hydropower, navigation, water use sectors and freshwater ecosystems among others (Laaha et al., 2016; Stahl et al., 2016).

~~Among the natural drivers of drought are~~A key natural driver of drought is persistent high-pressure systems leading to prolonged periods of low precipitation and/or high evapotranspiration (Tallaksen and Van Lanen, 2004). To ~~increase our knowledge of how drought characteristics might change in the future~~improve drought forecasts and projections, we therefore need a better understanding of the relation between the different types of drought and their large-scale atmospheric and oceanographic drivers. Stationary Rossby waves have been found to play an important role in the development of summer patterns of monthly surface temperature and precipitation variability across northern Eurasia, and appear to have led to the extreme heat wave and drought in 2003 and 2010 (Schubert et al., 2014, 2011). Kingston et al. (2015) found that the most widespread and long-duration meteorological droughts in Europe fall into two categories; northern European droughts with onset associated with an Atlantic ~~meridional dipole~~meridional-dipole atmospheric circulation anomaly similar to the North Atlantic Oscillation (NAO), and droughts elsewhere in Europe associated with anomalies related to a northeastward expansion of the Azores high ~~resembling~~, resembling an eastern Atlantic/western Russia (EA/WR) atmospheric circulation ~~patterns~~pattern. Fleig et al. (2011) investigated the relation between various circulation types and streamflow drought in Denmark and Great Britain, ~~and~~. They found that hydrological droughts ~~were~~are most frequently linked to circulation types representing a high-pressure system over the region affected by drought, which promote hydrological drought development by advection of warm dry air. In addition to stationary high and low-pressure systems, sea surface temperatures associated with large-scale climate modes of variability ~~are~~also have also been found to be important drivers for dryness and wetness variability over Europe (Ionita et al., 2015, 2012). In a study of streamflow drought in Great Britain, Kingston et al. (2013) found statistically significant SST and atmospheric anomalies linked to drought onset. The ~~study emphasises~~authors emphasise the shortcomings in the ability of circulation

indices (e.g. ~~such as~~ NAO) to capture fully the atmospheric variation preceding drought onsets, and highlights the value of composite analysis in developing an improved understanding of ocean-atmosphere-drought connections.

The 2018 event was unique in ~~its~~ the northern location of the high-pressure system initiating the drought, as compared to other major European drought events in the last decades (Ionita et al., 2017; Stahl, 2001). The affected Nordic region
5 (Norway, Denmark, Sweden and Finland) exhibits a high heterogeneity in terrestrial and hydroclimatological characteristics. Despite its rather limited size, the region spans several latitudes and has a pronounced west-east gradient in climate and topography, ranging from high mountains in the west to low-lying regions in the south and east. Prevailing westerly winds run northeastwards from the Atlantic, bringing abundant rainfall ~~in the western part. Orographic effect causes~~ along the west. Orographic effects lead to large local variability in precipitation in the ~~mountainous areas~~ western part of the region. Denmark,
10 southern Sweden, and western coast of Norway have a maritime climate, in contrast to the more continental climate in eastern Norway, Sweden and Finland. The landscape is largely affected by last glaciations, with typical landforms such as U-shaped valleys, fjords, and lakes~~and~~, as well as a large spatial heterogeneity in glacial deposits. Land cover varies from vast areas of bare rock and shallow deposits in the west and north, to undulating inland areas characterised by numerous lakes, forests and wetlands, and to areas in the south with thick soils and large aquifers (e.g. Sømme, 1960). Combined with the important effect
15 of seasonal snow on hydrology, varying with latitude and altitude, excluding the very south, the result is a high diversity in hydroclimatological conditions.

In depth analyses of historical drought events, what triggers them and how they manifest themselves in the hydrological cycle, ~~enables~~ enable us to increase our understanding of this complex phenomenon, which is vital to enhance drought forecasting, projection and mitigation. Motivated by these considerations, this paper focuses on characterizing ~~characterising~~ the
20 2018 drought in northern Europe in ~~detail, including exploring atmosphere-drought connections. The aim~~ a historical context. Traditionally, anomaly maps (in absolute or relative terms) have been used to characterise the meteorological situation of past European events and their spatiotemporal development. Recent examples include events such as the major European drought in 2003 (Black et al., 2004), 2010 (Barriopedro et al., 2011) and 2015 (Ionita et al., 2017). Ranking maps are another way of communicating the extremeness of an event in a long-term perspective, which is simple and easy to communicate
25 (e.g. Ionita et al., 2017). By ranking the events selected from a time series (e.g. one value each year) according to their magnitude (e.g. temperature), one can map the rank of a particular event, compared to all other years on record, across a region of interest. In this study, we embedded both these approaches; i.e., 2018 anomalies relative to a period of reference (1971–2000), and ranking maps for the 2018 event based on the 60-year period 1959–2018.

The aim of the study is twofold; 1) to investigate the extremeness of the 2018 situation and the accompanying meteorological
30 and hydrological drought in northern Europe, and 2) to identify ~~large-scale~~ large-scale atmospheric circulations associated with below normal summer streamflow in the Nordic region. The latter is investigated using Empirical orthogonal functions (EOFs), which is a well-known method to detect spatial patterns of variability and how they change with time. In Ionita et al. (2015), EOFs are used to study the variability in meteorological drought in Europe and its relationship to geopotential height, which is similar to the approach adopted here for the main patterns of summer streamflow variability.

The paper is organised as follows: The data and methods are described in Sect. 2 and 3, respectively. In Sect. 4 ~~the results shown and described for the~~ (Results), the 2018 meteorological situation (Sect. 4.1), meteorological drought (Sect. 4.2) and hydrological drought (Sect. 4.3) ~~as well as are presented, and~~ the relation between summer streamflow and large-scale atmospheric circulation investigated (Sect. 4.4). A detailed discussion is provided in Sect. 5, followed by the conclusion in Sect. 6.

5 2 Data

2.1 Meteorological data

Meteorological data used in this study ~~comprise~~ comprises the 500 mb geopotential height (HGT500), the zonal and meridional wind, sea surface temperature (SST), air temperature and precipitation. Monthly data of HGT500, and zonal and meridional wind, used to describe the atmospheric circulation, were extracted from the NCEP-NCAR 40-year reanalysis project (Kalnay et al., 1996). These datasets are available from 1948 to near-present, and have a global coverage on a $2.5^\circ \times 2.5^\circ$ longitude/latitude grid. SST data was extracted from the ~~National Centers for Environmental Information (NOAA) high-resolution Optimum Interpolation Sea Surface Temperature version 2 (OISSTv2; Reynolds et al., 2007). OISSTv2 consists~~ Hadley Centre Sea Ice and Sea Surface Temperature dataset (HadISST; Rayner et al., 2003), consisting of monthly SST from ~~September 1981–January 1805~~ to near-present on a global scale with a spatial resolution of $0.251^\circ \times 0.251^\circ$ longitude/latitude.

15 Europe-wide ($35.625\text{--}71.875^\circ$ N and $-10.875\text{--}41.625^\circ$ E) daily total precipitation and daily maximum, minimum and mean air temperature on a ~~0.25 regular latitude/longitude grid (used for the analysis described in Sect. 3.1 and 3.2), and daily total precipitation on a~~ 0.1° ~~regular latitude/longitude grid (used for the analysis described in Sect. 3.3)~~ regular longitude/latitude grid, were derived from the E-OBS dataset version ~~19-021.0e~~ (Cornes et al., 2018). The E-OBS ~~datasets are~~ dataset is based on the European Climate Assessment and Dataset station information (ECA&D), and ~~consist~~ consists of daily data from
20 01.01.1950 until near-present.

2.2 Hydrological data

Hydrological data ~~consists of~~ used includes time series of streamflow and groundwater levels from stations in the Nordic region. Streamflow measured at a given point reflects the accumulated responses to precipitation over space and time, whereas groundwater levels represent the lagged response in groundwater over an area varying with local conditions. Streamflow data
25 ~~stem stems~~ from gauges in Norway, Sweden, Denmark and Finland. Quality-controlled, daily observational streamflow time series ~~was were~~ provided by the Norwegian Water Resources and Energy Directorate (NVE) ~~for Norway~~, Danish Environment Portal for Denmark, Swedish Meteorological and Hydrological Institute (SMHI) ~~for Sweden~~, and Finnish Environmental Institute (SYKE) ~~for Finland~~. All gauges had near-natural catchments, i.e. ~~the streamflow is to a large degree unaffected by human interventions~~ limited or no human interventions (such as reservoirs or water abstractions) influencing the streamflow. Only
30 gauges having less than 10 days with missing values between May–September each year in the 60-year period 01.01.1959–31.12.2018, were chosen.

The resulting dataset ~~consists~~ consisted of time series from 79 gauges, with catchment areas ranging from 6.6 km² to 10864 km² (median of 276 km²). Figure 1 shows the locations of the gauges as well as ~~their annual cycles and streamflow regimes.~~ ~~The streamflow regimes were based on the regime classification of the streamflow regime at each site, reflecting the typical streamflow variability over the year.~~ The regime classification was based on Gottschalk et al. (1979) and calculated for the period 1959–2018 (a detailed description of the classification procedure is provided in Appendix A1). The five regimes ~~reflect the typical streamflow variability in time,~~ are classified according to whether the streamflow is dominated by 1) winter high flow and summer low flow, mainly due to high evapotranspiration during summer (Atlantic regime), 2) winter low flow and spring high flow, due to snow accumulation and snowmelt (Mountain regime), or 3)–5) various combinations of these two patterns (Baltic, Transition and Inland regime). Three of the stations with a mountain regime (marked with crosses) experience high flow during late summer due to ~~the large presence of glaciers a high percentage~~ (>30 % of the catchment)) of glaciers in their catchments. Standardised monthly streamflow statistics for each station are shown in Fig. S3–S5 in the Supplement.

Observational–Observed time series of near-natural groundwater levels, i.e. data from stations with limited or no human influence (such as water abstractions), are even less accessible than streamflow data. This includes the necessary metadata with local site information. As a result, the groundwater analysis was limited to data from stations in Norway and Sweden, provided by NVE and the Geological Survey of Sweden (SGU), respectively. The time series were quality controlled at the host institutions, however, a visual inspection was performed to delete potential erroneous outliers. Groundwater level time series were generally shorter than the streamflow time series, and rather than a 60-year period as used for streamflow, a 30-year period (1989–2018) was selected as a balance between the number of stations and the record length.

The In a majority of the groundwater wells ~~had,~~ observations were taken on a weekly to monthly ~~temporal resolution basis~~ in most of the period ~~covered. In Norwegian wells.~~ In Norway, daily or sub-daily measurements ~~started at~~ were available from the beginning of the 21st century. Half of the Swedish wells had daily or sub-daily measurements from 2016 onwards, whereas the other half had a coarser temporal resolution ~~for the whole across the whole 30-year~~ period. Only groundwater stations with at least one monthly measurement during April–September over the ~~analysis period~~ 30-year period analysed, were selected. ~~The varying temporal resolution of the original measurements might affect the results. However, we argue that~~ groundwater Groundwater has in many cases ~~have~~ a slow response and thus ~~have valuable information content at the holds~~ valuable information at a monthly resolution (e.g. Hisdal and Tallaksen, 2000). Sub-daily measurements were aggregated into daily averages means, whereas days of missing data were filled by linear interpolation between the two adjacent measurements, following the method used by the National Hydrological Monitoring Programme in the UK (NHMP, 2017).

The final resulting groundwater dataset includes data groundwater level observations from 56 wells. Their locations, ~~annual~~ eyes and groundwater regimes are shown in Fig. 2. ~~The Several of the Swedish wells are closely located, sharing the same location name, however, representing different depths and soil types. These are plotted as pies of the same point. The number of wells represented by each site is given in the figure.~~ The groundwater regime classification ~~is based on the classification by Kirkhusmo (1988) was based on Kirkhusmo (1988),~~ using data for the period 1989–2018 (a detailed description of the classification procedure is provided in Appendix A2). Region I is characterised by low groundwater levels in late summer due to warm season evapotranspiration losses. Region III has a minima in late winter prior to the start of the snowmelt period,

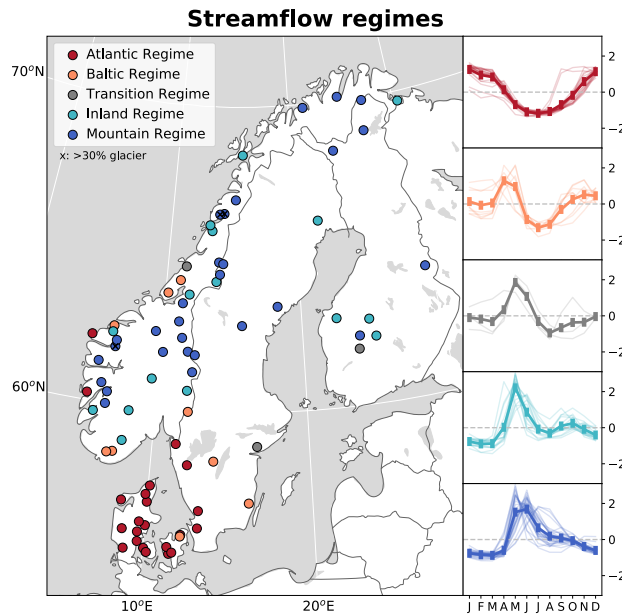


Figure 1. Locations and streamflow regimes (based on Gottschalk et al., 1979) of the 79 streamflow stations used in the study. The right panel shows plots of mean monthly standardized streamflow (i.e. subtracted the mean and divided by the standard deviation) hydrographs for each regime (indicated by thin lines) together with the regime mean hydrograph streamflow (bold line).

~~whereas Region I being a combination of the two, experiences two minima, one in late winter and one in late summer. Some of the wells are were classified as a delayed version of a regime due to slow-responding groundwater fluctuations. Standardised monthly groundwater level statistics for each well are shown in Fig. S6–S7 in the Supplement.~~

3 Methods

5 The variables, indices (including periods used) and spatial coverages used to characterise the 2018 meteorological situation, meteorological drought and hydrological drought, are summarised in Table 2. ~~Starting from~~ From looking at a large spatial domain, including Europe and its surrounding regions ~~when describing~~, when describing the main climate drivers, the analysis gradually "zooms in" on the Nordic region ~~that shows~~, which experienced the most extreme meteorological situation in spring and summer of 2018. Calculations were done for each month in 2018, however, the results mainly focus on the period

10 May–August.

3.1 Meteorological ~~Situationsituation~~

The extremeness of the meteorological situation for each month ~~in May–August 2018~~ was analysed using the sea surface temperature (SST), geopotential height at 500 mb (HGT500), daily maximum surface-air temperate (Tx) and precipitation

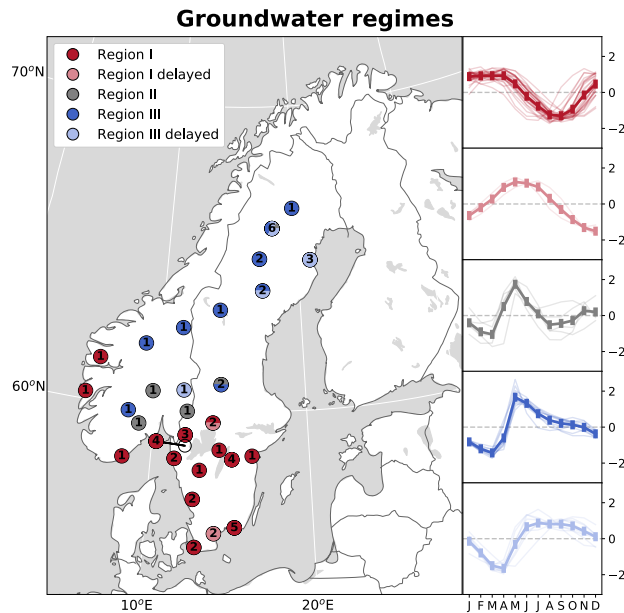


Figure 2. Locations and groundwater regimes (based on Kirkhusmo, 1988) of the 56 groundwater wells used in the study. The number on each point represents the number of stations at that location. To ease readability, one site with four wells in southwestern Sweden (red point on the map) is shifted to the left of, and pointing to, its real location. The right panel shows plots of mean monthly ~~standardized~~standardised (i.e. subtracted the mean and divided by the standard deviation) ~~hydrographs~~groundwater levels for each regime (indicated by thin lines) together with the regime mean ~~hydrograph~~groundwater levels (bold line).

(P). For HGT500 and SST, the 2018 anomalies (in meters and degree Celsius, respectively) relative to ~~a reference period~~the reference period 1971–2000 were computed for each month ~~May–August in the period~~May–August in the period over Europe and the surrounding regions. ~~For HGT500 we used the reference period 1971–2000, whereas for SST we used the reference period from the start of the dataset (in 1981) to 2000.~~In addition, ~~average-mean~~average-mean May–August HGT500 60-year (1959–2018) time series and corresponding 2018 anomalies (in standard deviations from the 60-year mean) were computed for each subdomain of 20° × 20° longitude/latitude throughout the European domain, i.e. the area 35° N–80° N and 12.5° W–42.5° E moving one grid cell (2.5°) at a time. This allowed the extremeness in the persistent high-pressure system for the whole May–August period to be estimated.

~~For~~The extremeness in temperature and precipitation ~~was analysed by ranking maps of each month in 2018.~~was analysed by ranking maps of each month in 2018. First, monthly mean ~~of~~of Tx and monthly total sums of P were computed for the 60-year period (1959–2018, ~~and monthly ranking maps of 2018 made for the six-~~), ~~and for each month the years were ordered from the most extreme~~and for each month the years were ordered from the most extreme (highest temperature and ~~six lowest precipitation.~~ six lowest precipitation. A ranking map for a specific year (here 2018) is made by first extracting the value of a variable of interest for each year in a chosen period (here 1959–2018), ~~order the sample from the most extreme lowest precipitation~~order the sample from the most extreme lowest precipitation to the least extreme value, ~~and find.~~and find. Then, ranking maps of 2018 were made by finding the position (rank) of ~~the specific year 2018 if it~~the specific year 2018 if it

were among the six highest temperatures (in the case of Tx) or six lowest precipitation totals (in the case of P). Similar maps were computed for the European 2015 drought by Ionita et al. (2017) using the period 1950–2015. In case of ties between years, 2018 was set as the least extreme of the years with equal values. This was done to avoid exaggerating the extremeness of 2018 in terms of precipitation totals, such as in some Mediterranean regions where it is not uncommon with months with zero precipitation. A rank of one ~~imply record-breaking implies~~ record-breaking high temperature (in the case of Tx) or low precipitation (in the case of P) in 2018, a rank of two indicates that 2018 had the second most extreme value in that month, etc. Here, temperature/precipitation with ranks of 1–6 are referred to as extreme. The ranks correspond to specific percentiles of the data, such that a rank of 3 or 6 ~~correspond~~ corresponds to the 5th or 10th percentile, respectively, when the period under investigation is 60 years.

10 3.2 Meteorological ~~Drought~~ drought indices

The meteorological drought of each month May–August 2018 was assessed using the Standardized Precipitation Index (SPI; McKee et al., 1993; Guttman, 1999) and the Standardized Precipitation Evapotranspiration Index (SPEI; Vicente-Serrano et al., 2010; Beguería et al., 2014). A ~~three-months~~ three-month accumulation period was chosen ~~for~~ in both cases (i.e. SPI3 and SPEI3) to reflect the seasonality in northern Europe (WMO, 2012).

15 SPI is recommended as a meteorological drought index for drought monitoring by the World Meteorological Organization (WMO and GWP, 2016). It is a widely used measure of precipitation anomalies that can be compared across locations with different climatology and highly non-normal precipitation distributions (Stagge et al., 2014). SPEI is a more recent drought index that measures ~~the normalized~~ normalised anomalies in the climatic water balance, defined as precipitation minus potential evapotranspiration (PET; Vicente-Serrano et al., 2010). As opposed to SPI, SPEI takes into account atmospheric variables other than precipitation that may affect drought. ~~Which additional atmospheric variables that are included~~ Additional atmospheric variables to include depend on the equation chosen to estimate PET. The Hargreaves equation (Hargreaves and Samani, 1985) was used in this study following the recommendation by Stagge et al. (2014). The Hargreaves equation estimates daily PET based on each day's mean temperature, the difference between daily minimum and maximum temperature (proxy for net radiation), and an estimate of (extraterrestrial) radiation based on the latitude and day of the year.

25 SPI3 (SPEI3) was computed by: 1) fitting ~~three-months accumulated precipitation~~ three-month accumulated P (or P-PET) in the reference period 1971–2000 to a parametric distribution, 2) transforming non-exceedance probabilities from the parametric distribution to the standard normal distribution, and finally, 3) using the normal distribution to estimate the 2018 anomaly in terms of standard deviations (Lloyd-Hughes and Saunders, 2002; Guttman, 1999; McKee et al., 1993). Both SPI and SPEI rely on the choice of a parametric distribution. This study ~~follows~~ followed the recommendations by Stagge et al. (2015) ;
30 ~~i.e. it uses to use~~ the gamma distribution for the SPI calculation, ~~incuding~~ including a "centre of mass" adjustment for zero precipitation periods, and the generalized extreme value distribution for the SPEI calculation. Except for differences in input data and transformation procedure to the standard normal distribution, the computation routine is the same for SPEI and SPI, and the multi-temporal nature and statistical interpretability of the two indices are therefore also the same (Stagge et al., 2014). SPI and SPEI were calculated using the R-package *SCI* developed by Gudmundsson and Stagge (2016).

Dry conditions are represented by negative SPI and SPEI values, and wet conditions by positive values. A ~~categorization~~ categorisation of SPI values is found in Lloyd-Hughes and Saunders (2002), defining SPI ~~absolute values of 1–1.5 values between -1 and -1.5~~ (9.2 % probability) as moderate drought/~~moderately wet, SPI absolute values of 1.5–2, SPI values between -1.5 and -2~~ (4.4 % probability) as severe drought/~~severely wet~~, and SPI ~~absolute values >2 values less than -2~~ (2.3 % probability) as extreme drought/~~extremely wet~~. ~~This categorization was used~~. Correspondingly, positive SPI values are categorised as moderately wet (1–1.5), severely wet (1.5–2) and extremely wet (>2). This categorisation was adopted for the interpretation of the SPI3 and SPEI3 results in this study.

3.3 Hydrological ~~Drought~~drought

The extremeness in streamflow and groundwater level was analysed by calculating the monthly means and ranking the ~~low~~ end-lowest values (low streamflow and low groundwater tables) for each month May–August in 2018, following the same procedure as for temperature and precipitation (Sect. 3.1). For streamflow, the ~~60-year~~ 60-year period 1959–2018 was used as a basis for the ranking, and thus the same percentile equivalents as for temperature and precipitation apply. A ~~30-year~~ 30-year period was used for groundwater due to the generally shorter time series. ~~In this case~~ Thus, a rank in groundwater of 3 or 6 ; ~~correspond~~ corresponds to the 10th or 20th percentile, respectively.

The response in groundwater to climatic input is often delayed and smoothed, however, the delay may vary greatly from site to site affecting the occurrence and duration of groundwater drought (Van Loon, 2015; Van Loon and Van Lanen, 2012). Here, the delay in groundwater response to precipitation was assessed, defined as the accumulation ~~time of the spatially collocated period (at daily resolution) of the nearest grid cell's daily~~ precipitation yielding the highest correlation between accumulated ~~daily~~ precipitation and daily groundwater levels for the period 1989–2018.

20 3.4 Empirical ~~Orthogonal Function Analysis~~ orthogonal function analysis and ~~Composite Maps~~ composite maps

Key patterns in ~~large-scale~~ large-scale atmospheric circulation associated with low and high summer streamflow in the Nordic region were analysed by computing the HGT500 anomalies for the years of high and low anomalies. The anomalies were identified by the three first principle components resulting from an empirical orthogonal function (EOF) analysis of the summer streamflow data. An EOF analysis allows insight into the most dominant modes of variability in a complex temporally and spatially varying dataset by decomposing the dataset into fixed spatial patterns (EOFs) with corresponding time series (principle components, PCs), ~~that each represent~~ each representing a given proportion of the total variance in the dataset (Wilks, 2006).

~~Summer~~ The magnitude of a given EOF loading gives the strength of the relationship between the summer streamflow time series and the corresponding PC. A negative EOF loading represent an inverse relationship between the summer streamflow time series and the corresponding PC, which can take on both negative and positive values. Mean summer (June-July-August) ~~streamflow averages~~ streamflows were computed for each year 1959–2018 and the time series ~~standardized~~ standardised and detrended prior to the empirical orthogonal function analysis. The ~~June–August period was chosen for the EOF analysis (rather than May–August, which is in focus in Sect. 3.1–3.3) to avoid the effect of high flow in May caused by snowmelt. Furthermore, EOF analysis and composite maps are traditionally done on a three-month seasonal basis, making the results more easily~~

comparable to other studies. The EOFs and PCs were calculated using the Python library *eofs* (Dawson, 2016). For each of the principle components (PCs), years with absolute values larger than one standard deviation were defined as high (positive values) and low (negative values) anomaly years. For each set, we computed "high years composite maps" and "low years composite maps" of concurrent (average-mean summer; June-July-August) and preceding (average spring; March-April-May)
5 HGT500 anomaly and SST anomaly anomalies. The significance of the composite maps were estimated by a two-sided standard t-test at a 5 % significance level.

4 Results

4.1 Meteorological Situationsituation

Figure 3a-d shows the evolution of SST anomalies from May–August 2018 as compared to the reference period (~~1981–2000~~ 1971–2000;
10 all months throughout 2018 are shown in Fig. A1). The strongest SST anomalies in the seas surrounding Europe in 2018 were found in May–September. Patterns of negative and positive SST anomalies are were relatively stable from ~~May–August~~ May–September, characterised by one negative and two positive anomalous SST centers. The strongest negative SST anomalies were found in an area south of Greenland (50–60° N), whereas strong positive SST anomalies were found below this area, in a belt from 20–80° W at approx. 40° N. The A second region of positive SST anomalies was found in the regions surrounding Europe
15 between 0–40° E (Barents Sea, Norwegian Sea, North Sea, Baltic Sea, ~~Balek-Black~~ Sea and parts of the Mediterranean Sea). The highest SST anomalies exceeded 4-3 °C and were found in the Baltic Sea, ~~Black-Sea and northeastern Mediterranean Sea.~~ Positive anomalies of similar magnitude were found in the Barents Sea in July and August.

HGT500 anomalies for each month May–August 2018 as compared to the reference period (1971–2000) are shown in Fig. 3e-h (all months throughout 2018 are shown in Fig. A2). May 2018 was characterised by a dipole-like structure in the
20 atmospheric circulation, with HGT500 anomalies ranging from -120 m to 120 m. A high-pressure system (anticyclonic circulation) was centred over Fennoscandia, whereas Greenland and eastern Canada were under the influence of a low-pressure system (cyclonic circulation). This represents a northwestern movement of the high and low-pressure systems present in April, when these were located over central/eastern Europe and the North Atlantic west of Ireland, respectively. South of the cyclonic circulation in May, a weaker anticyclonic circulation was ~~found-observed~~ over the east coast of the US. In June, the HGT500
25 anomalies were generally lower than in May, with anticyclonic conditions centred over the British Isles and at similar latitudes, two cyclonic circulations, one centred over the Canadian east coast and one centred over Russia at approx. 70° E. The HGT500 anomalies in July were similar to the ones in May in their spatial patterns and anomaly magnitudes, however, with a slight northward shift. In August, the high-pressure systems weakened in magnitude, with a high-pressure system located southeast of Fennoscandia, and a low-pressure system developed over the North Atlantic between Iceland and Norway. Similar
30 anomaly pattern and magnitudes persisted in September–October, before Fennoscandia again was under the influence of a strong high-pressure system in November and (too a lesser degree) December 2018.

The 2018 anomalies of the HGT500-averaged-over-the-period-mean May–August, ~~in 2018,~~ HGT500 relative to 1959–2018 (represented as standard deviations, std, from the 60-year mean) for a sequence of subdomains in Europe, are shown in Fig. 4a.

Each subdomain covers $20^{\circ} \times 20^{\circ}$ ~~lat longitude/lon, and they are shifted one grid cell (2.5) in longitudinal or latitudinal direction~~ at the time latitude. Results for each month May–August 2018 separately are shown in Fig. A3. Most of Europe ~~show~~ showed HGT500 values of more than 2 std, and in regions centred around Denmark (between -2.5 – 12.5° E and 52.5 – 57.5° N), HGT500 deviated more than 3 std. Figure 4b shows the aggregated May–August HGT500 time series for a selected subdomain centred over Scandinavia (Scandinavian subdomain: 52.5 – 72.5° N and 5 – 25° E), demonstrating ~~the record-breaking a record-breaking~~ high-pressure system ~~averaged~~ over the period May–August for this subdomain. As shown in Fig. A3, particular high anomalies ~~are seen~~ were observed in May and June, whereas more normal values ~~are~~ were found in June and August. In May 2018, the std ~~is~~ was twice as high as the second most extreme year (1993) and more than 3 std away from the mean.

Figure 5a–d shows the ~~ranks~~ top-six ranking of each month May–August 2018 (~~maximum~~) highest temperatures (all months throughout 2018 are shown in Fig. A4, and monthly anomalies in Fig. S1). Temperatures during this period were exceptionally high (~~rank 1–6~~), with record-breaking (rank 1) or near-record-breaking (rank 2–6) temperatures in several European regions. The most widespread extreme temperatures were found in May, when the ~~top six top-six~~ ranks (dominated by rank 1 and 2) covered almost the whole of the Nordic region and large parts of northern and eastern Europe. Record-breaking weather was reported by meteorological offices ~~in most of~~ across the affected countries. In Norway and Germany, for example, the meteorological institutes reported that the ~~national country average~~ May temperature was the highest on (the more than 100-year) record, and 97 meteorological stations in Norway (with record lengths between 15 and 155 years) registered record-breaking May temperature (Grinde et al., 2018b; Deutscher Wetterdienst, 2018). In June, the area covered by ~~exceptionally high extreme~~ temperatures decreased, mainly covering a smaller region from northern France to Poland, southern Scandinavia and the British Isles. Ireland ~~stands here out~~ stood out this month, with record-breaking temperatures. Only southern ~~Fennoscandia~~ ranked parts of Fennoscandia had ranks of 1–6 in June, however, this changed drastically in July, when almost the whole of Fennoscandia experienced the highest, or second highest, temperatures on the record ~~for this month~~. In Norway, 43 ~~measuring meteorological~~ stations broke their mean July temperature record (Grinde et al., 2018c). High ranks ~~are~~ were also seen in regions facing the North Sea and the Baltic Sea. A southern shift ~~is~~ was seen in August, ~~where~~ when a southwest-eastern belt of ~~exceptionally high extreme~~ temperatures extended from the Iberian Peninsula to southeastern Fennoscandia. Regions, mainly in Spain, Portugal and Germany, experienced record-breaking temperatures this month. Extreme temperatures were also observed in the months before and after May–August 2018 (mainly in April, September and October), covering regions south of Fennoscandia. In November, temperatures in northern and western Fennoscandia were again extremely high.

Record-breaking, or near-record-breaking, low precipitation for each month May–August (Fig. 5e–h; ~~rank of~~ all months are shown in Fig A5, and monthly anomalies in Fig. S2) were much less common and only found in smaller and more scattered areas across northeastern Europe. Some ~~however more extreme, localised extreme~~ clusters were found in June ~~mainly located,~~ mainly in southern UK, Benelux, Germany and Belarus. In July, larger clusters ~~are seen in most of~~ were seen covering Benelux, Denmark, parts of Fennoscandia and Germany. A relatively large region north of the Black Sea, including Moldova and parts of Romania, Ukraine and Russia, experienced record-breaking and near-record-breaking, low precipitation in August. In addition, smaller clusters of ~~exceptional extremely~~ low August precipitation were found in central Europe. Apart from May–August, scatters of record-breaking or near-record-breaking low precipitation in 2018 were mainly found in southwestern, central and

southeastern Europe. Exceptions are February and November, when larger parts of northern/northeastern Europe experienced extremely low precipitation.

4.2 Meteorological ~~Drought~~drought

SPI3 and SPEI3 for each month May–August 2018 are shown in Fig. 6 (all months are shown in Fig A6 for SPI3 and Fig A7 for SPEI3). From a slow development at the start of the year, a meteorological drought manifested itself (as indicated by SPI3 indicates moderate meteorological drought (SPI3<-1) in parts of Europe across a larger region north of 45° N in May, with a few scattered areas of severe meteorological drought (SPI3<-1.5) April and May. The situation worsened to peak in July when 1718 % of the grid cells had SPI3<-1.5. The most extreme meteorological drought in northern Europe (SPI3<-2) was found in July in a region surrounding Denmark, including southern Norway, Sweden, Benelux and Germany. Regions within the British Isles and the Baltic countries also recorded extreme meteorological drought this month. In August, extreme conditions persisted in Germany and neighboring countries, whereas the meteorological drought in Fennoscandia, the Baltic countries and the British Isles generally lessened (or ceased)as compared to July. Dry conditions persisted in central Europe, and extended to southern and eastern parts of Europe in September–November. Eastern and southeastern parts of Fennoscandia were again affected by moderate drought in November–December, after three months of only scatters of moderate drought in this region.

The year started rather wet across Europe in terms of SPI3, with wet conditions persisting in southeastern Europe until May. SPI3 also revealed extreme wet conditions (SPI3>2) on the fringe of the drought affected area, i.e. along the coastal regions in northern Norway (June–October) and southern parts of Europe, notable the Iberian Peninsula in May (March–May) and southeastern Europe in July and August (February–April and July–August). The SPEI3 shows showed a similar spatial pattern as SPI3, although somewhat higher anomalies are seen at the start of the period, i.e. were seen in May and June , for SPEI3, with 1011 %, respectively 1516 % of the grid cells in severe or extreme drought (i.e. values<-1.5) as compared to 57 % (May) and 113 % (June) for SPI3.

4.3 Hydrological ~~Drought~~drought

The 60-year ranking of monthly lowest (top-six) ranking of lowest monthly streamflow in 2018 in the Nordic region (Norway, Sweden, Finland and Denmark) revealed record-breaking or near-record-breaking low streamflow in several regions from June, peaking in July , and persisting in southeastern area of the region in August (Fig. 7a–d,), Ranks of all months in 2018 are shown in Fig. A8) , and standardised monthly hydrographs for 2018 are shown in Fig. S3–S5. In May, only two (3 %) of the stations experienced extremely low streamflow (rank of 1–6). In June, however, 46 % of the stations had extremely low streamflow, and 13 % were record-breaking. The proportion of stations with extremely low streamflow expanded to 68 % in July (28 % were record-breaking). Extreme conditions persisted in the southeastern area of the region (mainly eastern Denmark, southeastern Sweden and southern Finland throughout 2018.) until the end of the year.

The 30-year ranking of monthly lowest (top-six) ranking of lowest monthly groundwater levels in Sweden and Norway for each month May–August 2018 are shown in Fig. 7e–h (all months are shown in Fig A9, and monthly standardised groundwater

tables can be found in Fig. S6–7). Four (7 %) of the stations in Norway and Sweden had extremely low groundwater levels (rank of 1–6) in May 2018. In June, 43 % of the stations had a rank of 1–6 (7 % were record-breaking), expanding to 55 % (14 % record-breaking) in July and 63 % (14 % record-breaking) in August. Ranks between 1 and 6 ~~are~~ were seen in 38–54 % of the wells until the end of 2018. Extremely low groundwater levels did not show any distinct spatial patterns. In several cases, stations located close to each other (pies of the same point) showed different results, reflecting the importance of local conditions in determining the groundwater level.

The delay in groundwater response to precipitation ~~varies~~ (as defined in Sect. 3.3) varied among the study sites from 30 to 1500 days (Fig. 8a), whereas mean groundwater levels ~~below surface~~ (measured from the surface) ranged from 0.36–13.4 m (median of 2.16 m; Fig. 8b). With one exception, the most extreme groundwater levels in Norway in June and July 2018 (in terms of ranks), were found for ~~the~~ locations with the fastest response time (, i.e. 30–90 days). Figure 8c shows the ~~groundwater ranks between 1 and 6~~ top-six groundwater ranks for each month throughout 2018, plotted with the response delay along the x-axis and the mean groundwater level depth (Fig. 8b) along the y-axis. Extreme groundwater levels emerged in June in the most shallow wells (less than 3 meters depth from surface), followed by deeper wells in July–August, with response delays of up to 400 days in July–August. In September, the most shallow wells with the fastest response showed less extreme ranks, whereas deeper and more slowly responding wells started to experience extreme conditions. This pattern continued throughout 2018.

4.4 Relation between ~~Summer-Streamflow~~ summer streamflow and ~~Large-Scale Atmospheric Circulation~~ large-scale atmospheric circulation

The three first principle components of the EOF analysis ~~explain~~ explained 52 % of the detrended and ~~standardized~~ standardised summer streamflow variability over the period ~~1959–2018~~ 1959–2018, and their time series and loadings are shown in Fig. 9. ~~Note that for negative EOF loadings, the corresponding PC time series is relevant with the opposite sign. The larger the absolute value of an EOF loading, the more important is the corresponding PC time series in explaining the summer streamflow behavior of a given station.~~ EOF1 explains explained 23 % of the variability and ~~is most~~ was mostly relevant for the streamflow in the western and northern part of Norway ~~-(Fig. 9a)~~. EOF1 ~~is~~ was also relevant for some stations in Denmark, which ~~are~~ were characterised by high flow when stations in Norway ~~have had~~ low flow and vice versa. In summer 2018, PC1 was close to one standard deviation higher than the ~~time-series average~~ time series mean (Fig. 9d), reflecting dry conditions in western and northern Norway. Similar to EOF1, EOF2 explains explained 21 % of the summer streamflow variability ~~-(Fig. 9b)~~. EOF2 ~~is~~ was mostly relevant for the streamflow in Denmark, southeastern Norway and southwestern Sweden. The PC2 time series ~~indicate~~ indicated extreme low flow conditions in summer 2018 in these regions ~~-(Fig. 9e)~~. A smaller amount of variability (8 %) ~~is~~ was explained by EOF3 ~~-(Fig. 9c)~~. EOF3 ~~reflects~~ reflected opposite summer streamflow conditions in the west (Norway and Denmark) relative to the east (easternmost Norway, Sweden and Finland). The PC3 value for 2018 ~~is~~ was close to the ~~time-series average~~ time series mean (Fig. 9f), and thus the conditions represented by EOF3 and PC3 ~~are~~ were not relevant for the summer 2018.

Summers of low and high streamflow were related to the prevailing large-scale atmospheric circulation by extracting the summer HGT500 of ~~high and low~~ low and high anomaly years from the three first PCs time series from the summer streamflow EOF analysis. Years with absolute PC values larger than one standard deviation from the times series ~~average-mean~~ were defined as high (positive values) and low (negative values) anomaly years. Summer (June–August) HGT500 composites for these years along with wind directions and significance, are shown in Fig. 10.

Summer low flow in western and northern Norway as indicated by high PC1 values ~~are~~, was associated with a high-pressure system centred over the Norwegian Sea and covering most of Fennoscandia, and a low-pressure system centred over the British Isles and over Russia at approx. 60° E. In summers with low PC1 values, western and northern parts of Fennoscandia ~~lies~~ lie on the border between a low-pressure system in the north and a high-pressure system in the south. ~~The years~~ Years of high (low) PC2 values ~~are~~ were associated with a low-pressure (high-pressure) system over the North Sea, flanked by a high-pressure (low-pressure) system on the central part of the ~~north Atlantic basin~~ North Atlantic and over Russia. These pressure systems ~~cover~~ covered the region with the largest EOF2 loadings, with summer high flow associated with cyclonic circulation, and summer low flow associated with the an ~~anti-cyclonic~~ anticyclonic circulation over the region. A high-pressure system ~~over~~ centered over southern Scandinavia and a low-pressure system over Russia at approx. 40° E ~~are~~ were observed for summers of high PC3 values, and a low-pressure system over the North Sea and southern Scandinavia ~~is typical~~ for summers with low PC3 values.

5 Discussion

The 2018 extreme drought centred in northern Europe, substantially affected the Nordic region, particularly in late spring and summer before moving southwards in August. The Nordic region has widely different hydroclimatological and terrestrial characteristics as compared to ~~the more commonly affected drought regions of~~ other recently drought-affected regions, such as southern and central Europe ~~in 2003 and 2015~~. This makes the drought of 2018 and its propagation in the hydrological cycle unique. Special for the region is a high diversity in hydroclimatological conditions, including the effect of snow on hydrology. Accordingly, the response to a meteorological drought and its propagation in the hydrological cycle will vary. Here, we discuss the 2018 drought, first from a climatological perspective (Sect. 5.1), then by ~~the hydrological perspective~~ considering its hydrological footprint (Sect. 5.2). Further, the results of the EOF analysis, linking atmospheric circulation and low summer streamflow in the Nordic region, are discussed (Sect. 5.3), followed by some final remarks on the ~~representability~~ representativity of the hydrological data used in the study (Sect. 5.4).

5.1 The 2018 drought from a climatological perspective

The 2018 drought ~~confirms~~ confirmed the central role of anticyclones in the development of northern (>40° N) Eurasian droughts (~~Schubert et al., 2014~~) as highlighted by Schubert et al. (2014). The strongest HGT500 anomalies over the period ~~May to August~~ May–August were found in May and July. May was characterised by a cyclonic circulation centred over Greenland and western Russia, and pronounced anticyclonic circulation centred over the continental Nordic region ~~extending~~

~~down to central North Atlantic~~, extending south to central North Atlantic and the east-coast of North America. This wave train pattern resembles the atmospheric circulation associated with the leading mode of drought variability over Europe as presented by Ionita et al. (2015). Large parts of the region experiencing anticyclonic conditions in the months from ~~May to August~~May–August 2018, also showed extreme temperatures (defined as having a rank between 1 and 6). The stronger the

5 HGT500 anomaly, the more extreme the temperature, emphasising the strong link between the two variables.

Overall, the observed positive SST anomalies in summer 2018 ~~overlap~~overlapped spatially with the anticyclonic ~~circulations~~circulation (positive HGT500 anomalies) in May and July 2018. Anomalous anticyclonic circulation, as observed in these two months, ~~may~~ decrease convection and increase incoming solar radiation, leading to warmer SST in the underlying seas (Feudale and Shukla, 2011). The spatial pattern of SST anomalies in 2018 are similar to those in the summers of 2003 and 2015, repre-

10 senting two of the most extreme drought events in Europe in recent years (~~Ionita et al., 2017; Laaha et al., 2016; Black et al., 2004~~) (Ionita et al., 2017; Laaha et al., 2016; Fischer et al., 2007b; Black et al., 2004). During all three events, a persistent negative anomaly was centred south of Greenland over the period May–August. The anticyclonic centres and associated temperature extremes over continental Europe in 2018, were generally located more towards the northeast as compared to the 2003 and 2015 events. An overlapping region in central Europe experienced temperature extremes all three summers(~~Ionita et al., 2017; Fischer et al., 2007~~

15 . Overall, most major European streamflow droughts between 1960–90 were associated with high-pressure systems across central Europe (Stahl, 2001), highlighting the unique location of the 2018 event. This is especially the case for May and July, ~~in~~ which when the high-pressure system centred over the Nordic region ~~is was~~ more than 3 std, respectively 2 std, away from the 60-year mean (Fig. A3). However, in August 2018, the ~~hot temperature extremes covered~~region of extreme temperature moved southeast, covering a region extending from the southwest to northeast Europe, resembling the affected region in summer of

20 2015 (and to a lesser degree 2003).

Monthly precipitation extremes across the period May–August were not as widespread as temperature extremes, however, areas with extreme low precipitation (rank between 1 and 6), generally also experienced extreme high temperatures. Overall, the region affected was located further north as compared to previous large-scale droughts in Europe, such as the summer droughts in 2003 and 2015 (Ionita et al., 2017). The SPI3 and SPEI3 both showed ~~a~~ similar northern European located ~~drought, however,~~

25 ~~as both these indices dry anomalies. These indices both~~ reflect a 3-month accumulated deficit in precipitation, respectively a climatic water deficit, and thus a higher consistency is seen in time. Furthermore, both indices ~~show~~showed widespread dry conditions already in ~~May, reflecting the April, reflecting~~ conditions in the months ~~March–May~~February–April. As seen in Fig. A4, extreme high temperatures ~~are were~~ seen already in April in ~~parts of the region (central Europe), potentially leading~~large parts of Europe, which potentially led to drier than normal conditions in the soils.

30 For both SPI3 and SPEI3, the ~~drought peaks~~spatial extent of severe and extreme drought peaked in July.

Overall, the percentage of grid cells showing extreme drought ~~is was~~ higher for SPEI3, highlighting the importance of looking not only at precipitation when analysing the impact of drought, as ~~also previously recognized when comparing the SPI and SPEI for Europe (e.g. Stagge et al., 2017). already recognised by Stagge et al. (2017).~~ The use of potential evapotranspiration in SPEI (rather than actual evapotranspiration) ~~might may~~ be less an issue in the Nordic region, where evapotranspiration in

35 general is limited by energy, as opposed to water-limited areas dominating in central and southern Europe (McVicar et al.,

2012). The inclusion of potential evapotranspiration in SPEI (as opposed to using only precipitation in SPI), ~~might therefore prove suitable~~ may therefore prove acceptable for drought assessments in energy-limited regions. However, water may become a limiting factor ~~also~~ in these regions in exceptional years, such as the summer of ~~2018–2018~~ (Buitink et al., 2020). As the soil dries out, it may give rise to a positive land-atmosphere feedback, i.e. an enhanced warming is seen as less energy is spent
5 on evapotranspiration. Such soil moisture-temperature feedbacks have played an important role in the evolution of previous European heat waves (Fischer et al., 2007a), and may have played an important role in the 2018 event as well. Being outside the scope of this study, this would be an interesting aspect of a further study.

5.2 The 2018 drought from a hydrological perspective

Overall, drought impacts are commonly related to deficits in different components of the hydrological cycle, not in the meteorological variables as such. Key impacts of the 2018 drought were related to soil moisture (crop failure and wild fires) and hydrological drought (e.g. impacts on energy, water supply and aquatic ecosystems). As ~~the a~~ drought propagate, the event is normally lagged, attenuated and lengthened as compared to the original meteorological event (Van Loon and Van Lanen, 2012; Van Loon et al., 2011), ~~the question being to what degree, which will.~~ The degree to which this happens vary with event and region impacted. Furthermore, antecedent water storage (initial conditions), such as snow, glaciers and groundwater, ~~play~~ plays
15 an important role in the occurrence, timing and development of ~~the a~~ hydrological drought.

In regions affected by seasonal snow, drought occurrence and propagation is to a large degree influenced by the snow ~~storage volume~~ and snowmelt timing as compared to a normal year. During the snow accumulation season in 2018, above normal precipitation fell in early winter in most of the Nordic region, and less than normal precipitation in western/northern Norway and Finland towards the end of the snow season (as indicated by SPI3; Fig. A6a–c). Most of the snow-dominated catchments (with the exception of the northernmost part of the Nordic region), experienced meteorological drought in May–
20 July. Record high temperatures ~~emerging~~ emerged during the snowmelt season (i.e. in May), and 19 stations (24 %), all with a mountain or inland regime, experienced one of their six highest May streamflow since 1959. For ~~the~~ other stations affected by snowmelt, however, a more normal flood situation followed ~~;~~ (Fig. S4–5); one hypothesis being that part of the snow was lost due to sublimation. In addition, higher than normal evapotranspiration rates led to less water feeding the streams. The high
25 snowmelt and evapotranspiration rates likely caused an earlier end of the snowmelt season as well as a smaller total volume of melt water contribution to streamflow compared to normal (given the same preconditions). Following the snowmelt peak, streamflow drought started emerging in June in large parts of the Nordic region. Noteworthy exceptions ~~are~~ were the three glacier dominated streamflow stations (Fig. S5), for which high summer temperatures led to high melt rates and sustained water contribution from the glaciers.

30 Streamflow stations without a snow season are mainly located in Denmark and southern Sweden. Denmark Extreme temperatures were found in part of this region in April, extending to the whole region in May. In southern Sweden, meteorological and hydrological drought developed from May, and record-breaking low streamflow seen from June. Most of Denmark, on the other hand, did not experience a meteorological drought until July, ~~despite extreme temperatures in May~~. Accordingly, streamflow drought was first observed in July and (to a lesser degree) August, ~~;~~ However, this was only seen for stations located

in the ~~eastern-southeastern~~ parts of Denmark. ~~Most of the stations in western Denmark, however,~~ Stations in western and northern Denmark did not experience extremely low streamflow at all during May–August 2018. As a whole, Denmark had extremely low precipitation and severe to extreme meteorological drought, as indicated by SPI3, in July. ~~The spatial pattern of~~ A southeastern-northwestern gradient in extreme temperature (and SPEI3) this month, however, reflects the ~~east-west deviation~~ in spatial pattern of extremely low streamflow in Denmark, indicating that higher than usual evapotranspiration rates likely ~~has~~ contributed to extreme conditions in the ~~east. In the west, on the other hand, persisted groundwater contribution to streamflow combined with southeast.~~ Correspondingly, less extreme evapotranspiration ~~losses may in the west and north might~~ have prevented streamflow drought to develop there.

Whereas ~~exceptional-extremely low streamflow~~ conditions sustained in the southeastern area of the Nordic region (~~eastern~~ southeastern Denmark, southeastern Sweden and southern Finland) throughout 2018, streamflow in the north and western part of the region was replenished by ~~heavy precipitation in August (Grinde et al., 2018a):~~ high precipitation totals in August (Fig. S2h). This divide reflects the southeastern movement of the anticyclonic circulation as well as the cyclonic circulation over the Norwegian Sea in August, ~~and winds moving northeast with winds~~ from the North Sea, bringing precipitation towards the coast ~~along with them.~~ The precipitation did not only replenish the rivers and end the streamflow drought, but led to extremely wet conditions at several streamflow stations ~~-(Fig. S3–5).~~ Western and northern stations experienced one of their six highest monthly streamflow since 1959 in August (~~5-five~~ stations), September (21 stations) and October (16 stations). ~~Accordingly, the streamflow drought ends in August in western and northern part of the Nordic region, whereas in the~~ In the southeastern area, extreme ~~conditions persisted for several stations~~ streamflow conditions persisted towards the end of ~~the~~ 2018. Extreme conditions reappeared in November, even affecting stations that did not experience extremely low streamflow during the summer. This can be explained by continued below normal precipitation in September–October (Fig. S2), and a new high-pressure system over northeastern Europe in November leading to extremely low precipitation and severe to extreme meteorological drought in large parts of the southeastern Nordic region.

The groundwater wells were all located in ~~the area-areas~~ affected by moderate to extreme meteorological drought, as indicated by SPEI3, in May, June, July and (to a lesser degree) August. ~~However, a high local variability is seen for groundwater drought (rank between 1 and 6), reflecting neither the spatial pattern of meteorological drought, extremely low streamflow, nor the span in groundwater regimes.~~ The high spatial variability in hydrogeological properties across the Nordic region is mirrored in the diversity in groundwater response to meteorological conditions, as reflected in a high local variability for groundwater drought (rank between 1 and 6) even for closely located wells. Except for four wells that experienced low groundwater levels already from March, no wells showed groundwater drought in May. Similar to streamflow, this ~~is was~~ likely due to wet preconditions, such as high groundwater levels and/or snow volumes recharging groundwater during the melt season ~~-(Fig. S6–7).~~ In June, extreme conditions ~~are were~~ found among the most shallow groundwater wells, probably due to high evapotranspiration rates in combination with precipitation deficits. From July onwards, extreme conditions ~~are were~~ found in wells of increasing depth and response time. The extreme conditions first started to cease in the shallowest and fast responding wells from September. At the end of the year, 38 % of the wells still experienced extreme conditions, and below normal groundwater levels persisted well into 2019 (e.g. Table 1,n). Similar to streamflow, this was likely a combined effect of a delay in

the hydrological system, a continued below normal precipitation, and meteorological drought associated with a high-pressure system establishing over northeastern Europe in November.

5.3 ~~Atmospheric Circulation Associated~~ circulation associated with ~~Low Summer Streamflow~~ low summer streamflow in the Nordic ~~Region~~ region

5 The EOF analysis revealed that more than half (52 %) of the variability in summer streamflow ~~-, over the period 1959–2018,~~ in the Nordic ~~regions~~ region (1959–2018), can be explained by the three first principle components, whereof the two first EOFs ~~explain~~ explained 44 % (Fig. 9). The analysis ~~is was~~ somewhat biased towards Danish conditions, as the station density ~~is was~~ much higher here compared to the rest of the region, in particular Sweden and Finland. EOF1 and EOF2 ~~indicate a division~~ indicated two distinct patterns in summer streamflow variability ~~between;~~ in western/northern Norway ~~and (EOF1) and in~~ the southeastern part of the Nordic region (EOF2). During 1959–2018, ~~only two summers had summer low flow~~ low summer streamflow in the whole region ~~(only occurred twice, i.e. 1969 and 2006). These two summers are also previously identified as 2006. These summers have also previously been identified as exceptionally~~ dry by different drought indices (e.g. Spinoni et al., 2015; Hannaford et al., 2011), and ~~are years with overlying here found to correspond to~~ May–August HGT500 anomalies of more than 1 std above the 1959–2018 ~~average mean~~ average mean (Fig. 4).

15 High values of summer PC1 ~~indicate~~ indicated low summer streamflow in the northwestern part of the Nordic region, and ~~are were~~ associated with a ~~high pressure~~ high-pressure system over the Norwegian Sea (Fig. 10). Several of the streamflow stations with strong EOF1 loadings recorded extremely low streamflow values in June and July 2018. However, the summer of 2018 was not a high anomaly year in PC1, which might be due to the ~~heavy high~~ precipitation in August 2018 replenishing the rivers ~~in this region~~.

20 Low values of PC2 ~~indicate~~ indicated low summer streamflow in the southeastern part of the Nordic region, with the summer of 2018 as the most extreme year. ~~The main reason for this might be the extreme~~ This may result from the extreme streamflow conditions throughout June–August at several of the stations that ~~have had~~ the strongest EOF loadings along the Sweden-Norway border and southern Sweden (Fig. 7b–d). ~~After Following~~ 2018, the most extreme low anomaly years, as indicated by PC2, ~~are were~~ 1975–76. This period has previously been identified as benchmark drought event in western and northern Europe (e.g. Zaidman and Rees, 2000; Stahl, 2001). Low values of PC2 ~~are were~~ also associated with a high-pressure system over the North Sea, surrounded by low-pressure systems over Greenland/~~north~~ North Atlantic, Russia and the Mediterranean region. The pattern has some resemblance with the Scandinavian teleconnection pattern (SCAN). Interestingly, May 2018 ~~has~~ had the highest May SCAN value (of 1.69) and July 2018 the third highest July SCAN value (of 2.27, the highest being 2.61 from 1997) over the period 1950–2019 (data from https://climexp.knmi.nl/data/icpc_sca.dat, retrieved 14.04.2020).

30 5.4 Hydrological data ~~representativity~~ representativity

The streamflow dataset ~~used in this study~~ covers a rather wide range of catchments areas (6.6–10864 km²), and includes stations across all of Norway, Denmark, Sweden and Finland. However, the density of stations varies, being much higher in Denmark

and Norway as compared to Sweden and Finland. This lack of spatial representation affects the EOF analysis in particular, but also the percentages of stations with extremely low streamflow.

The number of wells included in the groundwater dataset was strongly limited by the requirement of no/little human influence (or lack of knowledge thereof), data quality and the period defined. The selected groundwater wells are relatively shallow, with a median depth of 2.16 m below surface, however, the range across the region or average value is not known, thus it is difficult to state whether this is a representative set of wells or not. Nevertheless, the large span in the 'delay in groundwater response' variable suggests a good coverage. The groundwater dataset only covers Sweden and (southern) Norway, and as much as 46 of the 56 stations are located in Sweden, thus the results ~~would be~~ are biased towards Swedish conditions. In addition, several of the well wells are located at the same site, often at different depth depths, affecting the spatial ~~representativity~~ representativity of the dataset. ~~However~~ Nevertheless, these wells highlight confirm the high local variability seen in the groundwater level response, reflecting the local heterogeneity in hydrogeological properties, ~~and thus cautions the local relevance of conclusions regarding groundwater drought made at the regional scale~~. Accordingly, this calls for caution when drawing conclusions at a regional scale based on local groundwater data.

6 Conclusions

This study characterised the 2018 northern European drought from both a climatological and hydrological perspective. This event was unique in its northern location, affecting a region with highly diverse ~~hydrometeorological~~ hydroclimatological conditions compared to the more central and southern parts of Europe, recently hit by major droughts such as the events of 2003 and 2015.

The North Atlantic ~~Ocean~~ and seas surrounding Europe experienced persistent anomalously high SST from May–August and record-breaking temperatures over the Nordic region in May and July, which were associated with record-breaking high-pressure systems overlying the region. Extreme monthly precipitation deficits were not as wide spread as ~~the~~ extreme monthly temperatures, however the persistent lack of precipitation from May–July led to extreme meteorological drought (estimated by SPI3) in a region surrounding Denmark, including southern Norway, Sweden, Benelux and Germany. The meteorological drought in this region was ~~considered even~~ found more extreme when considering the climatic water balance (~~precipitation minus potential evapotranspiration~~) using the estimated by SPEI3 index, emphasising the importance of accounting for temperature (and not solely precipitation as in SPI) in meteorological drought assessments. After July, the high-pressure system shifted southward, ~~centred in~~ and centred over Germany, and meteorological drought was only seen in small clusters across the Nordic region.

Whereas record-breaking temperatures and moderate meteorological drought emerged over most of the Nordic region in May, hydrological drought (estimated as monthly ranks between 1–6 of streamflow and groundwater) did not appear before June. ~~The effect of snow is an important hydrological characteristic~~ Snow plays an important role over large parts of the region, and at many locations the streamflow were still fed by meltwater during May 2018. The number of stations experiencing extremely low streamflow (rank between 1 and 6) expanded from 43 % in June to 68 % in July. Stations with more than

30 % of their catchment covered by glaciers did not experienced streamflow drought during the summer due to the ~~continuous~~ contribution of glacial melt water. In mid-August, ~~heavy precipitation~~ high precipitation totals replenished rivers in western and northern parts of the Nordic region, whereas extremely low streamflow persisted throughout 2018 in ~~the~~ southeastern parts. Groundwater drought peaked in August with 63 % of the stations experiencing extremely low groundwater levels (rank 5 between 1 and 6). The spatial ~~pattern and temporal patterns~~ of groundwater drought ~~as it developed was were~~ heterogeneous, and an interpretation of the patterns ~~only first~~ made sense when looking at the groundwater depth and ‘~~response delay~~ delay in groundwater response to precipitation’ combined. Extremely low groundwater levels emerged in the shallowest wells in June. With time, extreme conditions were found in wells of increasing depth and response delay, and by the end of 2018, 38 % of the wells ~~still~~ had extreme low groundwater levels. The high local variability observed in the development of groundwater drought 10 in 2018, highlights the care and awareness needed when analysing groundwater drought at the regional scale based on local well data ~~that varies in depth and with different~~ site characteristics.

The leading modes of Nordic summer streamflow variability (~~1959–2018 revealed a distinction~~) revealed two distinct patterns in summer streamflow variability ~~between~~; one in the western/northern part and one in the southeastern part of the region. As identified by composite maps of summer geopotential height anomalies, high-pressure systems centred over the 15 Norwegian Sea and the North Sea were associated with low summer streamflow in the western/northern and southeastern part of the Nordic region, respectively. In both cases, significant high-pressure systems ~~overlay overlaid~~ the region experiencing low summer streamflow, emphasising the important link between streamflow variability and large-scale atmospheric circulation.

The complexity of the 2018 drought event as revealed by the large variability in drought characteristics seen across space and time in the Nordic region, serves as yet another example of the care needed when analysing drought in different com- 25 ponents of the hydrological cycle. The diversity, caused by high local variability in terrestrial properties, ~~implies a different response~~ reflects different responses to the meteorological forcing and thus, different footprints of meteorological and hydrological drought. As the majority of drought impacts are felt on the ground, and thus more directly related to hydrology than meteorology, it is important to incorporate variables other than weather alone, when characterising drought.

Data availability. Our study is based on third party data. Citations to the datasets are included in the reference list, and data providers are 25 acknowledged in the acknowledgment section.

Author contributions. SJB, MI and LMT designed the study. MI performed the analysis and visualization of the geopotential height anomalies, and SJB performed the analysis and visualization of the remaining. SJB and LMT prepared the original draft. All authors reviewed and edited the final manuscript.

Competing interests. The authors declare that they have no conflict of interest.

Acknowledgements. Data providers are greatly acknowledged. HadISST data was obtained from <https://www.metoffice.gov.uk/hadobs/hadisst/> and are © British Crown Copyright, Met Office, 2020, provided under a Non-Commercial Government Licence <http://www.nationalarchives.gov.uk/doc/non-commercial-government-licence/version/2/>. NCEP-NCAR 40-year reanalysis project data was obtained from <ftp://ftp.cdc.noaa.gov/Datasets/ncep.reanalysis.derived/pressure/>. We acknowledge the E-OBS dataset from the EU-FP6 project UERRA (<http://www.uerra.eu>) and the Copernicus Climate Change Service, and the data providers in the ECA&D project (<https://www.ecad.eu>) ~~NOAA High Resolution SST data was provided by the NOAA/OAR/ESRL PSD, Boulder, Colorado, USA, from their Web site at <https://www.esrl.noaa.gov/psd/>.~~

We thank the Norwegian Water Resources and Energy Directorate (NVE), Danish Environment Portal for Denmark, Swedish Meteorological and Hydrological Institute (SMHI) and Finnish Environmental Institute (SYKE) for providing streamflow data for Norway, Denmark, Sweden and Finland, respectively. We also thank NVE and the Geological Survey of Sweden (SGU) for providing groundwater data for Norway and Sweden, respectively. Funding by the AWI Strategy Fund Project - PalEX and by the Helmholtz Climate Initiative - REKLIM are gratefully acknowledged. This paper supports the work of the UNESCO-IHP VIII FRIEND programme and the Panta Rhei Initiative of the International Association of Hydrological Sciences (IAHS).

References

- Barker, L. J., Hannaford, J., Chiverton, A., and Svensson, C.: From meteorological to hydrological drought using standardised indicators, *Hydrology and Earth System Sciences*, 20, 2483–2505, 2016.
- Barriopedro, D., Fischer, E. M., Luterbacher, J., Trigo, R. M., and García-Herrera, R.: The hot summer of 2010: redrawing the temperature
5 record map of Europe, *Science*, 332, 220–224, 2011.
- Beguiría, S., Vicente-Serrano, S. M., Reig, F., and Latorre, B.: Standardized precipitation evapotranspiration index (SPEI) revisited: parameter fitting, evapotranspiration models, tools, datasets and drought monitoring, *International Journal of Climatology*, 34, 3001–3023, 2014.
- Black, E., Blackburn, M., Harrison, G., Hoskins, B., and Methven, J.: Factors contributing to the summer 2003 European heatwave, *Weather*,
10 59, 217–223, 2004.
- Bordi, I., Fraedrich, K., and Sutera, A.: Observed drought and wetness trends in Europe: an update, *Hydrology and Earth System Sciences*, 13, 1519–1530, 2009.
- Buitink, J., Swank, A. M., van der Ploeg, M., Smith, N. E., Benninga, H.-J. F., van der Bolt, F., Carranza, C. D., Koren, G., van der Velde, R., and Teuling, A. J.: Anatomy of the 2018 agricultural drought in The Netherlands using in situ soil moisture and satellite vegetation
15 indices, *Hydrology and Earth System Sciences Discussions*, pp. 1–17, 2020.
- Buras, A., Rammig, A., and Zang, C. S.: Quantifying impacts of the 2018 drought on European ecosystems in comparison to 2003, *Biogeosciences*, 17, 1655–1672, 2020.
- Changnon, S.: Detecting drought conditions in Illinois, Illinois State Water Survey, Champaign, Illinois, USA, Circular, 169, 1–36, 1987.
- Cornes, R. C., van der Schrier, G., van den Besselaar, E. J., and Jones, P. D.: An Ensemble Version of the E-OBS Temperature and Precipitation Data Sets, *Journal of Geophysical Research: Atmospheres*, 123, 9391–9409, <https://doi.org/10.1029/2017JD028200>, 2018.
- Dawson, A.: eofs: A library for eof analysis of meteorological, oceanographic, and climate data, *Journal of Open Research Software*, 4, 2016.
- Deutscher Wetterdienst: Monatlicher Klimastatus Deutschland Mai 2018, Tech. rep., Deutscher Wetterdienst, www.dwd.de/DE/derdwd/bibliothek/fachpublikationen/selbstverlag/selbstverlag_node.html, 2018.
- Feudale, L. and Shukla, J.: Influence of sea surface temperature on the European heat wave of 2003 summer. Part I: an observational study,
25 *Climate dynamics*, 36, 1691–1703, 2011.
- Fischer, E. M., Seneviratne, S. I., Lüthi, D., and Schär, C.: Contribution of land-atmosphere coupling to recent European summer heat waves, *Geophysical Research Letters*, 34, 2007a.
- Fischer, E. M., Seneviratne, S. I., Vidale, P. L., Lüthi, D., and Schär, C.: Soil moisture–atmosphere interactions during the 2003 European summer heat wave, *Journal of Climate*, 20, 5081–5099, 2007b.
- 30 Fleig, A. K., Tallaksen, L. M., Hisdal, H., and Hannah, D. M.: Regional hydrological drought in north-western Europe: linking a new Regional Drought Area Index with weather types, *Hydrological Processes*, 25, 1163–1179, 2011.
- Gottschalk, L., Jensen, J. L., Lundquist, D., Solantie, R., and Tollan, A.: Hydrologic regions in the Nordic countries, *Hydrology Research*, 10, 273–286, 1979.
- Grinde, L., Heiberg, H., and Mamen, J.: Våret i Norge – Klimatologisk månedsoversikt August 2018, Tech. rep., Norwegian Meteorological
35 Institute, 2018a.
- Grinde, L., Kristiansen, S., and Mamen, J.: Våret i Norge – Klimatologisk månedsoversikt Mai 2018, Tech. rep., Norwegian Meteorological Institute, 2018b.

- Grinde, L., Lundstad, E., Skaland, R., and Tajet, H. T. T.: Været i Norge – Klimatologisk månedsoversikt Juli 2018, Tech. rep., Norwegian Meteorological Institute, 2018c.
- Gudmundsson, L. and Stagge, J. H.: SCI: Standardized Climate Indices such as SPI, SRI or SPEI, r package version 1.0-2, 2016.
- Guttman, N. B.: Accepting the standardized precipitation index: a calculation algorithm 1, JAWRA Journal of the American Water Resources Association, 35, 311–322, 1999.
- Hannaford, J., Lloyd-Hughes, B., Keef, C., Parry, S., and Prudhomme, C.: Examining the large-scale spatial coherence of European drought using regional indicators of precipitation and streamflow deficit, *Hydrological Processes*, 25, 1146–1162, 2011.
- Hannah, D. M., Demuth, S., van Lanen, H. A., Looser, U., Prudhomme, C., Rees, G., Stahl, K., and Tallaksen, L. M.: Large-scale river flow archives: importance, current status and future needs, *Hydrological Processes*, 25, 1191–1200, 2011.
- Hargreaves, G. H. and Samani, Z. A.: Reference crop evapotranspiration from temperature, in: *Proceedings of the Winter Meeting of American Society of Agricultural and Biological Engineers*, pp. 96–99, 1985.
- Haslinger, K., Koffler, D., Schöner, W., and Laaha, G.: Exploring the link between meteorological drought and streamflow: Effects of climate-catchment interaction, *Water Resources Research*, 50, 2468–2487, 2014.
- Hirschi, M., Mueller, B., Dorigo, W., and Seneviratne, S. I.: Using remotely sensed soil moisture for land–atmosphere coupling diagnostics: The role of surface vs. root-zone soil moisture variability, *Remote Sensing of Environment*, 154, 246–252, 2014.
- Hisdal, H. and Tallaksen: Drought event definition, ARIDE Technical Report 6, University of Oslo, Norway, 2000.
- Ionita, M., Lohmann, G., Rimbu, N., Chelcea, S., and Dima, M.: Interannual to decadal summer drought variability over Europe and its relationship to global sea surface temperature, *Climate Dynamics*, 38, 363–377, 2012.
- Ionita, M., Boroneant, C., and Chelcea, S.: Seasonal modes of dryness and wetness variability over Europe and their connections with large scale atmospheric circulation and global sea surface temperature, *Climate dynamics*, 45, 2803–2829, 2015.
- Ionita, M., Tallaksen, L., Kingston, D., Stagge, J., Laaha, G., Van Lanen, H., Scholz, P., Chelcea, S., and Haslinger, K.: The European 2015 drought from a climatological perspective, *Hydrology and Earth System Sciences*, 21, 1397–1419, 2017.
- Kalnay, E., Kanamitsu, M., Kistler, R., Collins, W., Deaven, D., Gandin, L., Iredell, M., Saha, S., White, G., Woollen, J., et al.: The NCEP/NCAR 40-year reanalysis project, *Bulletin of the American meteorological Society*, 77, 437–472, 1996.
- Kerr, Y. H.: Soil moisture from space: Where are we?, *Hydrogeology journal*, 15, 117–120, 2007.
- Kingston, D. G., Fleig, A. K., Tallaksen, L. M., and Hannah, D. M.: Ocean–atmosphere forcing of summer streamflow drought in Great Britain, *Journal of Hydrometeorology*, 14, 331–344, 2013.
- Kingston, D. G., Stagge, J. H., Tallaksen, L. M., and Hannah, D. M.: European-scale drought: understanding connections between atmospheric circulation and meteorological drought indices, *Journal of Climate*, 28, 505–516, 2015.
- Kirkhusmo, L.: Groundwater fluctuation patterns in Scandinavia, NHP-report, pp. 32–35, 1988.
- Kumar, R., Musuza, J. L., Loon, A. F. V., Teuling, A. J., Barthel, R., Ten Broek, J., Mai, J., Samaniego, L., and Attinger, S.: Multiscale evaluation of the Standardized Precipitation Index as a groundwater drought indicator, *Hydrology and Earth System Sciences*, 20, 1117–1131, 2016.
- Laaha, G., Gauster, T., Tallaksen, L., Vidal, J.-P., Stahl, K., Prudhomme, C., Heudorfer, B., Vlnas, R., Ionita, M., Van Lanen, H. A., et al.: The European 2015 drought from a hydrological perspective, *Hydrology and Earth System Sciences*, 21, 3001–3024, 2016.
- Liu, Q., Reichle, R. H., Bindlish, R., Cosh, M. H., Crow, W. T., de Jeu, R., De Lannoy, G. J., Huffman, G. J., and Jackson, T. J.: The contributions of precipitation and soil moisture observations to the skill of soil moisture estimates in a land data assimilation system, *Journal of Hydrometeorology*, 19, 2018.

- Lloyd-Hughes, B. and Saunders, M. A.: A drought climatology for Europe, *International journal of climatology*, 22, 1571–1592, 2002.
- McKee, T. B., Doesken, N. J., Kleist, J., et al.: The relationship of drought frequency and duration to time scales, in: *Proceedings of the 8th Conference on Applied Climatology*, pp. 179–184, American Meteorological Society, Anaheim, CA, 1993.
- McVicar, T. R., Roderick, M. L., Donohue, R. J., Li, L. T., Van Niel, T. G., Thomas, A., Grieser, J., Jhajharia, D., Himri, Y., Mahowald, N. M., et al.: Global review and synthesis of trends in observed terrestrial near-surface wind speeds: Implications for evaporation, *Journal of Hydrology*, 416, 182–205, 2012.
- Mishra, A. K. and Singh, V. P.: A review of drought concepts, *Journal of hydrology*, 391, 202–216, 2010.
- NHMP (National Hydrological Monitoring Programme): *Hydrological Summary for the United Kingdom: October 2017*, Tech. rep., Centre for Ecology and Hydrology, Wallingford, United Kingdom, 2017.
- 10 Peters, E., Torfs, P., Van Lanen, H., and Bier, G.: Propagation of drought through groundwater—a new approach using linear reservoir theory, *Hydrological processes*, 17, 3023–3040, 2003.
- Rayner, N., Parker, D. E., Horton, E., Folland, C. K., Alexander, L. V., Rowell, D., Kent, E., and Kaplan, A.: Global analyses of sea surface temperature, sea ice, and night marine air temperature since the late nineteenth century, *Journal of Geophysical Research: Atmospheres*, 108, 2003.
- 15 Reynolds, R. W., Smith, T. M., Liu, C., Chelton, D. B., Casey, K. S., and Schlax, M. G.: Daily high-resolution-blended analyses for sea surface temperature, *Journal of Climate*, 20, 5473–5496, 2007.
- Schenk, H. J. and Jackson, R. B.: The global biogeography of roots, *Ecological monographs*, 72, 311–328, 2002.
- Schubert, S., Wang, H., and Suarez, M.: Warm season subseasonal variability and climate extremes in the Northern Hemisphere: The role of stationary Rossby waves, *Journal of Climate*, 24, 4773–4792, 2011.
- 20 Schubert, S. D., Wang, H., Koster, R. D., Suarez, M. J., and Groisman, P. Y.: Northern Eurasian heat waves and droughts, *Journal of Climate*, 27, 3169–3207, 2014.
- Seneviratne, S. I., Corti, T., Davin, E. L., Hirschi, M., Jaeger, E. B., Lehner, I., Orlowsky, B., and Teuling, A. J.: Investigating soil moisture–climate interactions in a changing climate: A review, *Earth-Science Reviews*, 99, 125–161, 2010.
- Sømme, A.: *A Geography of Norden: Denmark, Finland, Iceland, Norway, Sweden*, J.W. Cappelens Forlag, Oslo, 1960.
- 25 Spinoni, J., Naumann, G., Vogt, J. V., and Barbosa, P.: The biggest drought events in Europe from 1950 to 2012, *Journal of Hydrology: Regional Studies*, 3, 509–524, 2015.
- Stagge, J. H., Tallaksen, L. M., Xu, C., and Van Lanen, H.: Standardized precipitation-evapotranspiration index (SPEI): Sensitivity to potential evapotranspiration model and parameters, *Proceedings of FRIEND-water*, pp. 367–373, 2014.
- Stagge, J. H., Tallaksen, L. M., Gudmundsson, L., Van Loon, A. F., and Stahl, K.: Candidate distributions for climatological drought indices (SPI and SPEI), *International Journal of Climatology*, 35, 4027–4040, 2015.
- 30 Stagge, J. H., Kingston, D. G., Tallaksen, L. M., and Hannah, D. M.: Observed drought indices show increasing divergence across Europe, *Scientific reports*, 7, 14 045, 2017.
- Stahl, K.: *Hydrological drought: A study across Europe*, Ph.D. thesis, Institut für Hydrologie der Universität, <http://www.hydrology.uni-freiburg.de/publika/band15.html>, 2001.
- 35 Stahl, K., Kohn, I., Blauhut, V., Urquijo, J., De Stefano, L., Acácio, V., Dias, S., Stagge, J. H., Tallaksen, L. M., Kampragou, E., et al.: Impacts of European drought events: insights from an international database of text-based reports, *Natural Hazards and Earth System Sciences*, 16, 801–819, 2016.

- Tallaksen, L. M. and Van Lanen, H. A.: Hydrological drought: processes and estimation methods for streamflow and groundwater, vol. 48, Elsevier, 2004.
- Tallaksen, L. M., Hisdal, H., and Van Lanen, H. A.: Space–time modelling of catchment scale drought characteristics, *Journal of Hydrology*, 375, 363–372, 2009.
- 5 Van Lanen, H. A., Laaha, G., Kingston, D. G., Gauster, T., Ionita, M., Vidal, J.-P., Vlnas, R., Tallaksen, L. M., Stahl, K., Hannaford, J., et al.: Hydrology needed to manage droughts: the 2015 European case, *Hydrological Processes*, 30, 3097–3104, 2016.
- Van Loon, A. F.: Hydrological drought explained, *Wiley Interdisciplinary Reviews: Water*, 2, 359–392, 2015.
- Van Loon, A. F. and Van Lanen, H. A.: A process-based typology of hydrological drought, *Hydrology and Earth System Sciences*, 16, 1915, 2012.
- 10 Van Loon, A. F., van Lanen, H. A., Tallaksen, L. M., Hanel, M., Fendeková, M., Machilica, M., Sapriza, G., Koutroulis, A., van Huijgevoort, M. H., Bermúdez, J. J., et al.: Propagation of drought through the hydrological cycle, Tech. rep., European Commission, 2011.
- Vicente-Serrano, S. M., Beguería, S., and López-Moreno, J. I.: A multiscale drought index sensitive to global warming: the standardized precipitation evapotranspiration index, *Journal of climate*, 23, 1696–1718, 2010.
- Vicente-Serrano, S. M., Lopez-Moreno, J.-I., Beguería, S., Lorenzo-Lacruz, J., Sanchez-Lorenzo, A., García-Ruiz, J. M., Azorin-Molina, C.,
15 Morán-Tejeda, E., Revuelto, J., Trigo, R., et al.: Evidence of increasing drought severity caused by temperature rise in southern Europe, *Environmental Research Letters*, 9, 044 001, 2014.
- Vidal, J.-P., Martin, E., Franchistéguy, L., Habets, F., Soubeyroux, J.-M., Blanchard, M., and Baillon, M.: Multilevel and multiscale drought reanalysis over France with the Safran-Isba-Modcou hydrometeorological suite, *Hydrology and Earth System Sciences Discussions*, 14, 459–478, 2010.
- 20 Wilks, D. S.: *Statistical Analysis in the Atmospheric Sciences*, London: Academic Press, 2006.
- WMO (World Meteorological Organization): Standardized precipitation index user guide, 2012.
- WMO (World Meteorological Organization) and GWP (Global Water Partnership): *Handbook of Drought Indicators and Indices*, World Meteorological Organization and Global Water Partnership, Geneva, Switzerland, 2016.
- Yang, Y., Donohue, R. J., and McVicar, T. R.: Global estimation of effective plant rooting depth: Implications for hydrological modeling,
25 *Water Resources Research*, 52, 8260–8276, 2016.
- Zaidman, M. and Rees, H.: Spatial patterns of streamflow drought in Western Europe 1960–1995, Tech. rep., Technical Report to the ARIDE project, 2000.

Table 1. Reports and news articles about 2018 heat and drought related impacts. [The impact categories follow the EDII Impact categorisation \(Stahl et al., 2016\).](#)

Ref.	<u>Publisher</u> <u>Impact category</u>	Region	<u>Publisher</u>	URL (last access) <u>Last update</u> <u>updated</u> / <u>last accessed</u>)
a	<u>Wildfires</u>	<u>Europe</u>	Joint Research Centre, European Commission	<u>Europe</u> https://op.europa.eu/en/publication-detail/-/publication/435ef008-14db-11ea-8c1f-01aa75ed71a1/language-en (<u>29.11.18</u> / <u>24.03.20</u>) 29.11.18
b	<u>Agriculture and livestock farming</u>	<u>European Union</u>	<u>Agriculture and Rural Development</u> , European Commission	<u>European Union</u> https://ec.europa.eu/info/news/drop-eu-cereal-harvest-due-summer-drought-2018-oct-03_en (<u>31.10.19</u> / <u>24.03.20</u>) 31.10.19
c	<u>Reuters</u> <u>Agriculture and livestock farming</u>	European Union	(24.03.20) <u>Reuters</u>	www.reuters.com/article/us-europe-grains-analyst/analysts-cut-eu-wheat-crop-outlook-again-on-catastrophic-north-idUSKBN1KU15E (<u>09.08.18</u> / <u>24.03.20</u>)
d	<u>Euronews</u> <u>Agriculture and livestock farming (mainly)</u>	Europe	(24.03.20) <u>Euronews</u>	www.euronews.com/2018/08/10/explained-europe-s-devastating-drought-and-the-countries-worst-hit (<u>12.08.18</u> / <u>24.03.20</u>)
e	<u>Agriculture and livestock farming</u>	<u>Sweden</u>	Swedish Board of Agriculture	<u>Sweden</u> https://www2.jordbruksverket.se/download/18.21625ee16a16bf0cc0eed70/1555396324560/ra19_13.pdf (<u>16.04.19</u> / <u>24.03.20</u>) 16.04.19
f	<u>Norwegian Agriculture Agency</u> <u>Agriculture and livestock farming</u>	Norway	(24.03.20) <u>Norwegian Agriculture Agency</u>	www.landbruksdirektoratet.no/no/statistikk/landbrukserstatning/klimarelaterte-skader-og-tap/avlingssvikt-statistikk (<u>02.09.19</u> / <u>24.03.20</u>)
g	<u>Norwegian Water Resources and Energy Directorate</u> <u>Energy and industry</u>	Norway, Sweden, Finland	(24.03.20) <u>Norwegian Water Resources and Energy Directorate</u>	www.nve.no/Media/7385/q3_2018.pdf (<u>17.10.18</u> / <u>24.03.20</u>)
h	<u>Energy and industry</u>	<u>Norway</u>	newsinenglish.no	<u>Norway</u> (www.newsinenglish.no/2018/07/13/drought-blamed-for-high-electricity-rates/ (<u>13.07.18</u> / <u>24.03.20</u>) 13.07.18
i	<u>Handelsblatt</u> <u>Today</u> <u>Waterborne transportation</u>	Germany	(24.03.20) <u>Handelsblatt</u> <u>Today</u>	www.handelsblatt.com/today/companies/low-water-dwindling-rhine-paralyzes-shipping-transport/23695020.html?ticket=ST-3121873-yvfwqi1ee3yWiy3BK1Zv-ap4 (<u>27.11.18</u> / <u>24.03.20</u>)
j	<u>Reuters</u> <u>Waterborne transportation</u>	Hungary	(24.03.20) <u>Reuters</u>	27 www.reuters.com/article/us-europe-weather-hungary- shipping/water-levels-in-danube-recede-to-record-lows- hindering-shipping-in-hungary-idUSKCN1L71DH

Table 2. Variables, extremeness indices and spatial coverage used to characterise the 2018 meteorological situation, meteorological drought and hydrological drought. All indices are calculated on a monthly basis.

Variable(s)	Extremeness index	Spatial Coverage
<i>Meteorological situation</i>		
Sea Surface Temperature (SST)	2018 anomaly (in degree Celsius) relative to 1981–2000 <u>1971–2000</u>	Europe and surrounding regions
Geopotential Height at 500 mb (HGT500)	2018 anomaly (in meters) relative to 1971–2000	Europe and surrounding regions
Geopotential Height at 500 mb (HGT500)	2018 anomaly (in standard deviations from the mean) relative to 1959–2018 for European subdomains	Europe and surrounding regions
Maximum Temperature (Tx)	Rank of 2018 based on highest 1959–2018 maximum temperatures	Europe
Precipitation (P)	Rank of 2018 based on lowest 1959–2018 precipitation	Europe
<i>Meteorological drought</i>		
Precipitation	Three-months <u>Three-month</u> Standardized Precipitation Index (SPI3) of 2018 relative to 1971–2000	Europe
Precipitation, and Minimum, Maximum and Mean Temperature	Three-months <u>Three-month</u> Standardized Precipitation Evapotranspiration Index (SPEI3) of 2018 relative to 1971–2000	Europe
<i>Hydrological drought</i>		
Streamflow	Rank of 2018 based on lowest 1959–2018 streamflow	Norway, Sweden, Finland and Denmark
Groundwater	Rank of 2018 based on lowest 1989–2018 groundwater level	Norway and Sweden

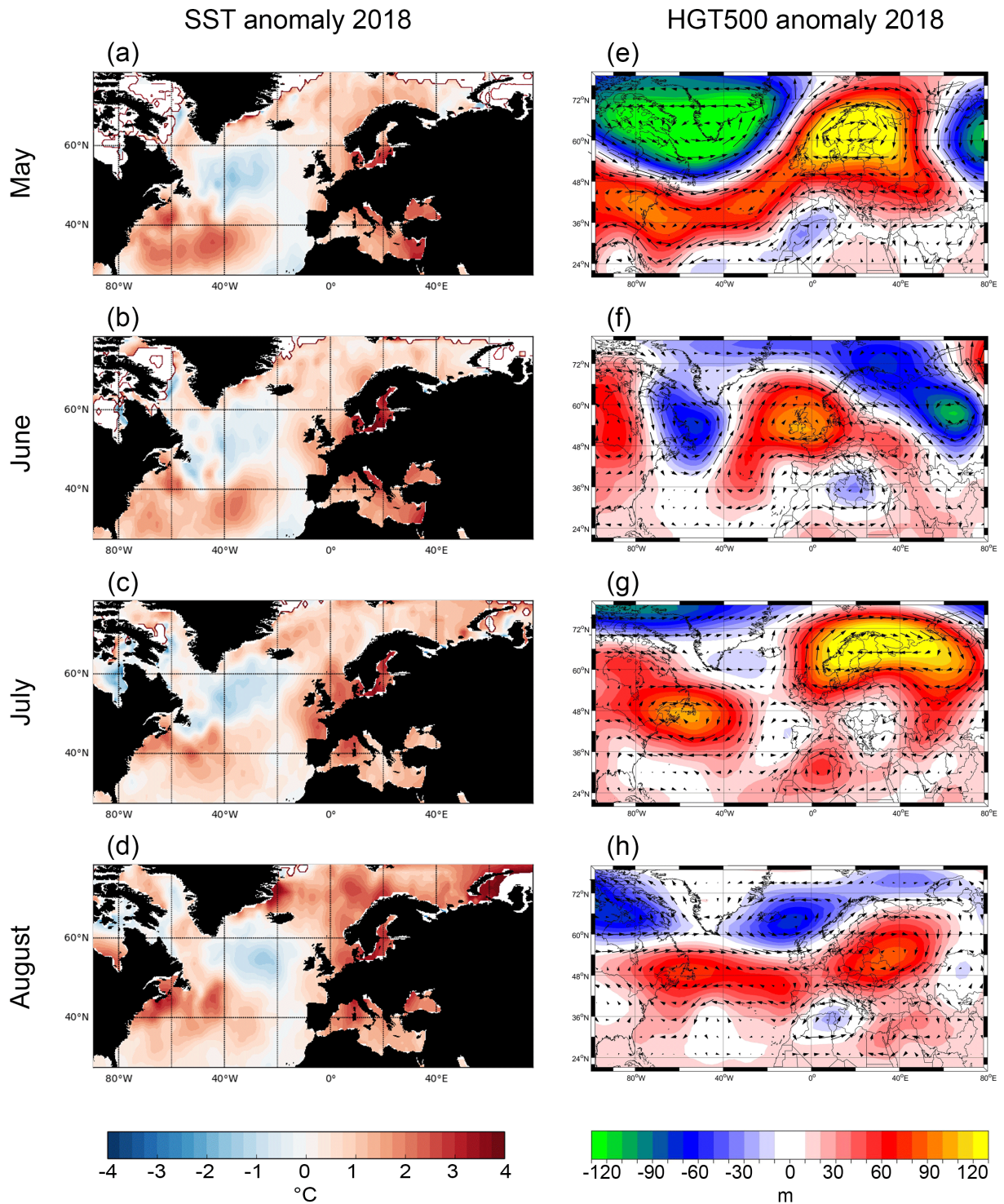


Figure 3. Left panel: Sea Surface Temperature (SST) anomalies for (a) May, (b) June, (c) July and (d) August 2018 relative to the reference period ~~1981–2000~~1971–2000. Right panel: Geopotential Height at 500 mb (HGT500) anomalies for (e) May, (f) June, (g) July and (h) August 2018 relative to the reference period 1971–2000. Zonal and meridional wind at 500 mb level are added to indicate wind directions.

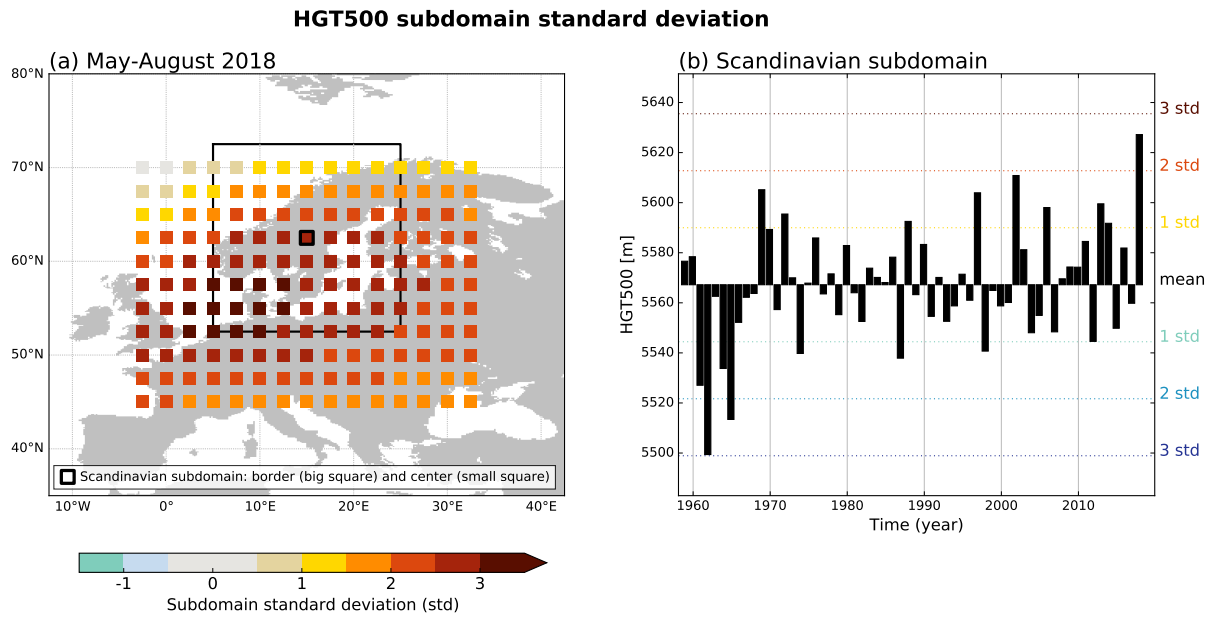


Figure 4. (a) Geopotential height at 500 mb (HGT500) shown as standard deviation (std) of aggregated May–August 2018 based on the 60-year period (1959–2018) for subdomains of 20° longitude/latitude throughout Europe, shifted 2.5° at a time. The coloured squares are the center points of each subdomain. This is illustrated for one subdomain over Scandinavia, with a large square and a small square marking the subdomain’s border and centerpoint, respectively. (b) Aggregated May–August HGT500 1959–2018 time series for the Scandinavian subdomain marked in (a).

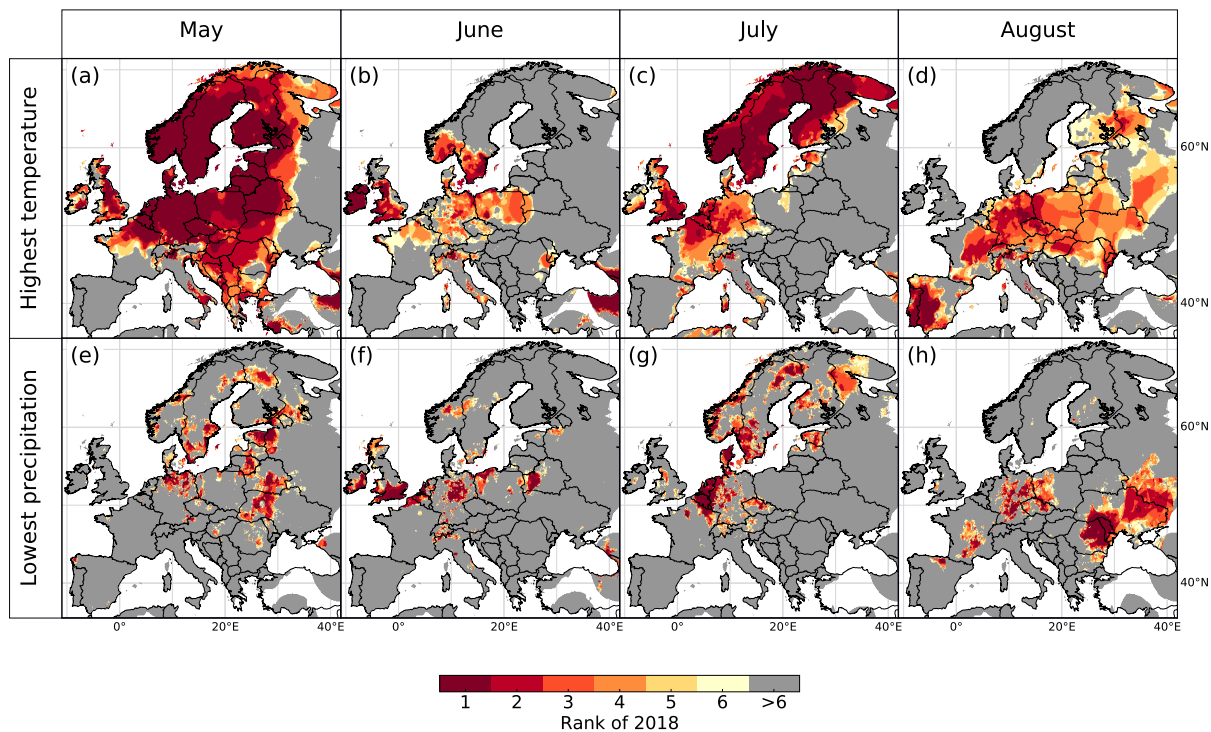


Figure 5. Top-six ranking of 2018 highest temperature (monthly mean of daily maximum temperature) for (a) May, (b) June, (c) July and (d) August, and top-six ranking of 2018 lowest precipitation for (e) May, (f) June, (g) July and (h) August. Analysed period is 1959–2018. A rank of one signifies that 2018 had the warmest (in the case of temperature) or driest (in the case of precipitation) month since 1959, a rank of two signifies that 2018 had the second most extreme value in that month, etc.

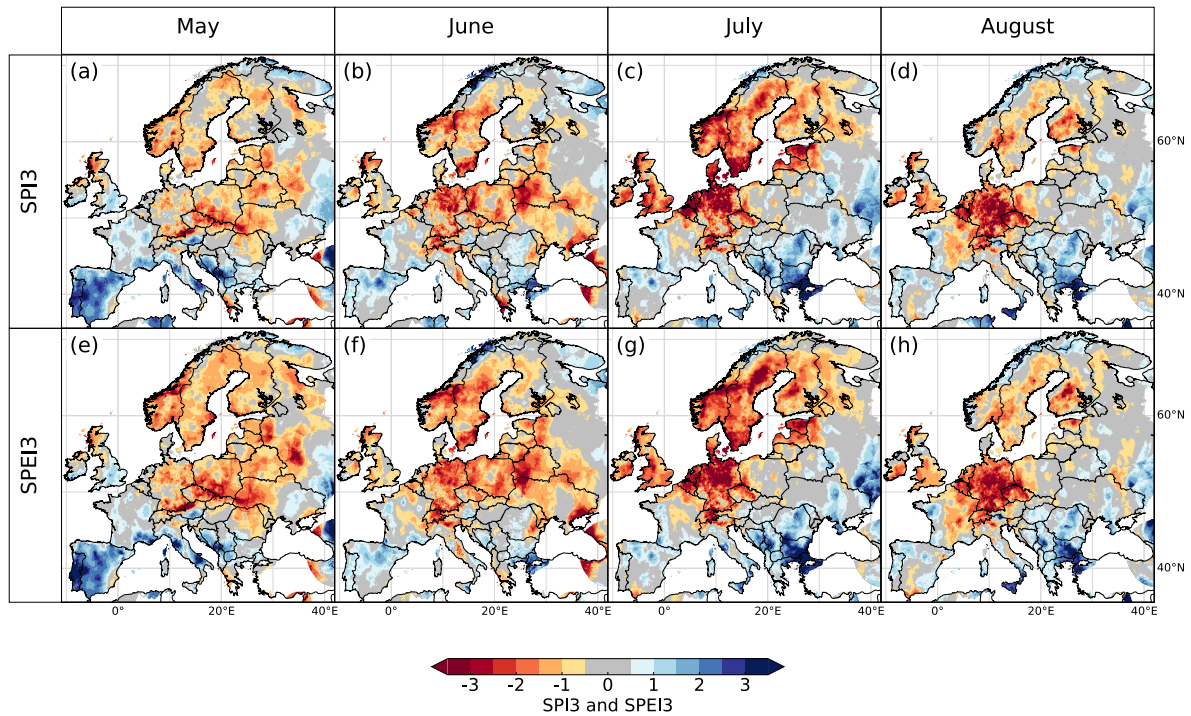


Figure 6. Meteorological drought 2018 indexed by SPI3 for (a) May, (b) June, (c) July and (d) August, and SPEI3 for (e) May, (f) June, (g) July and (h) August. Reference period used is 1971–2000.

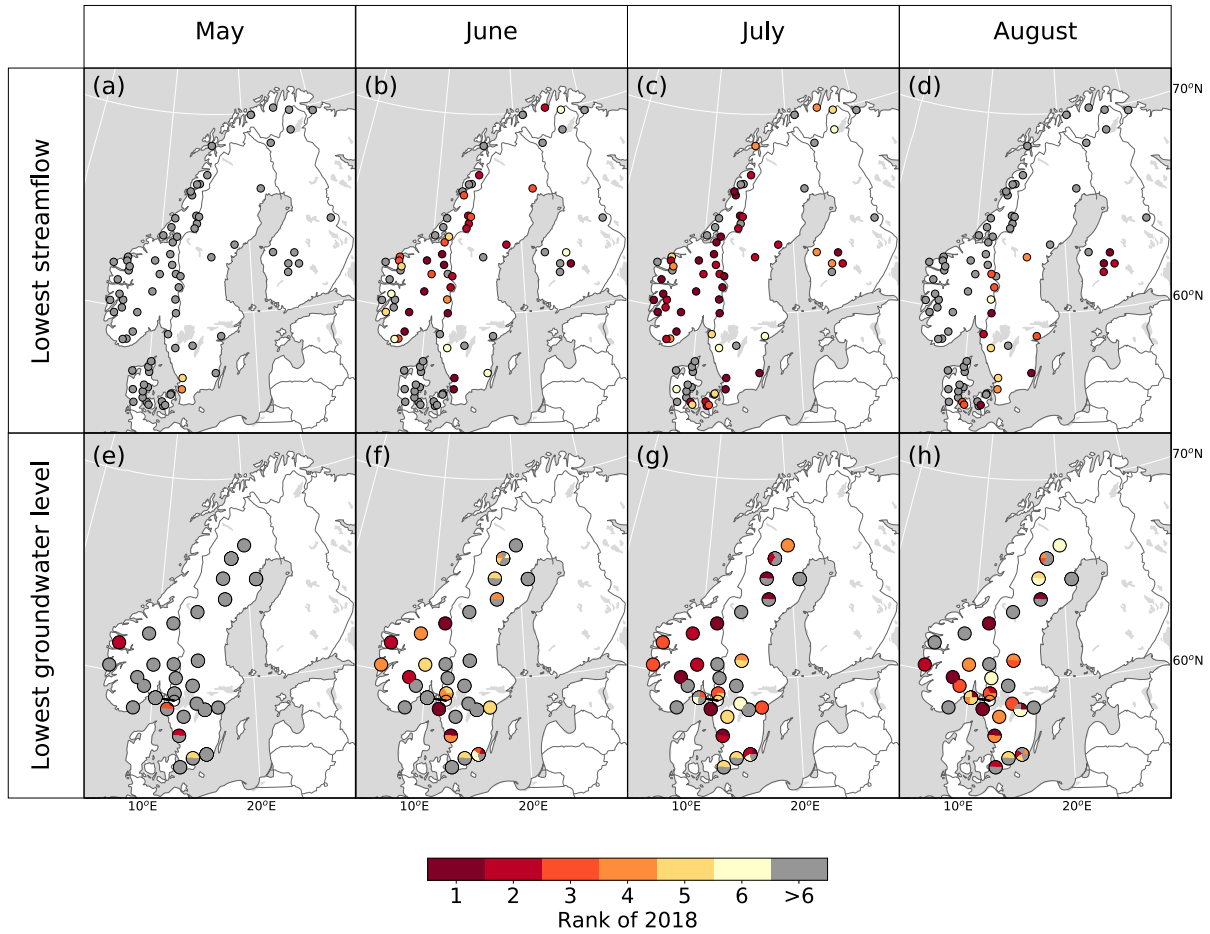


Figure 7. Top-six ranking of lowest streamflow for (a) May, (b) June, (c) July and (d) August, and top-six ranking of 2018 lowest groundwater level for (e) May, (f) June, (g) July and (h) August. Analysed period is 1959–2018 for streamflow and 1989–2018 for groundwater. A rank of one signifies that 2018 had the lowest monthly streamflow since 1959 (upper panel), or the lowest groundwater level in that month since 1989 (lower panel). A rank of two signifies that 2018 had the second most extreme value in that month, etc.

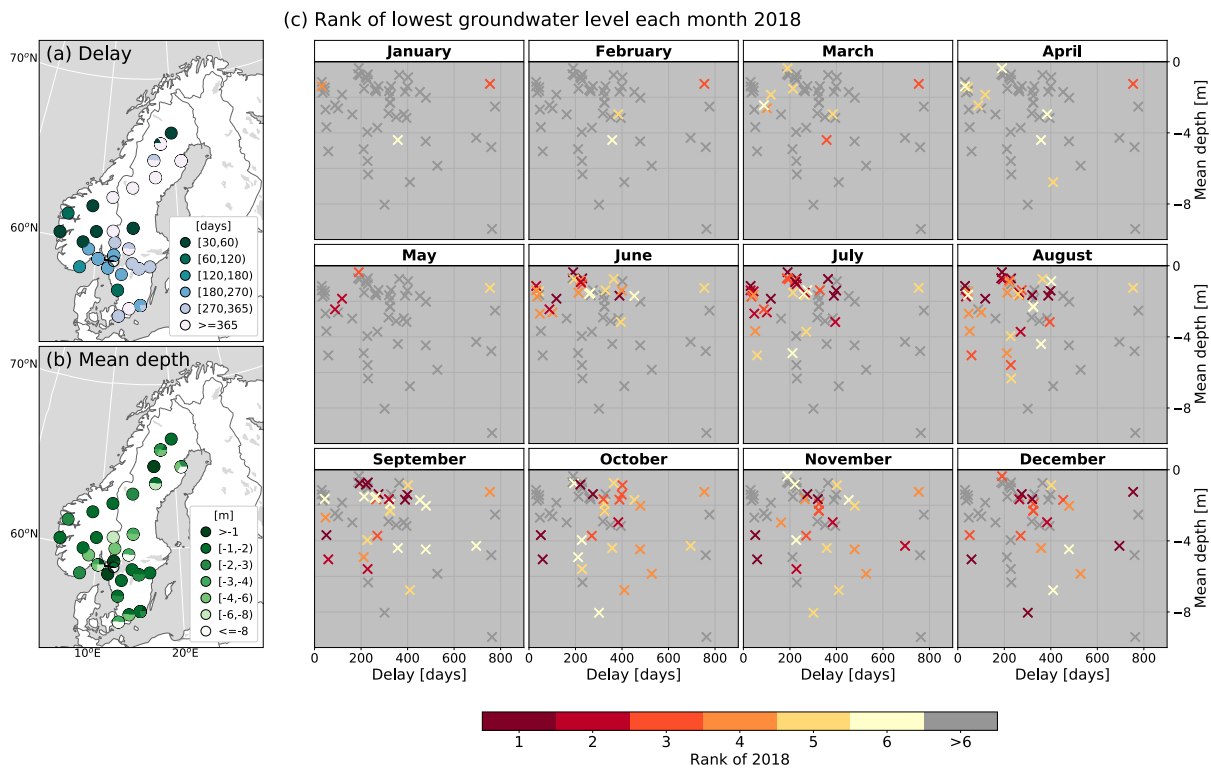


Figure 8. (a) [Groundwater-Delay in groundwater](#) response to precipitation, (b) mean 1989–2018 groundwater depth below surface, and (c) top-six ranking of lowest groundwater level in each month of 2018 plotted with each well’s delay and mean depth along the x-axis and y-axis, respectively. Two wells, one with delay of 1500 days and one with mean depth of -13.4 m, are outside the range of the ranking plots. Those two wells [have had](#) no rank of 1–6 in April–December 2018.

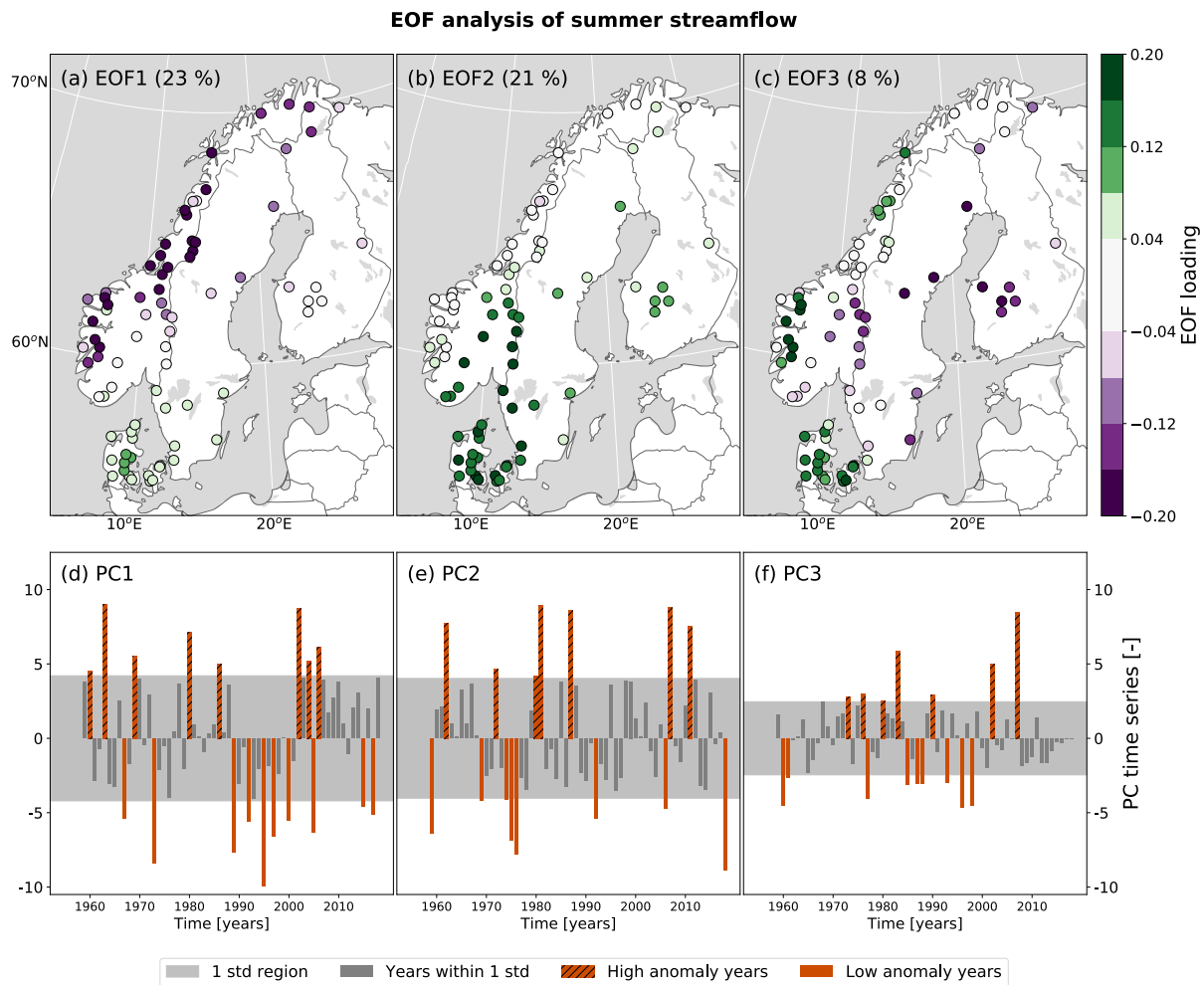


Figure 9. Empirical Orthogonal Function (EOF) analysis based on aggregated summer (June–August) ~~standardized~~ standardised and detrended streamflow (1959–2018). Maps (a–c) show the EOF loadings and time series (d–f) show the three first principle components (PCs). The explained variability of each mode is given in brackets in the corresponding EOF plot. For each of the PCs, years with absolute values larger than one standard deviation (std) are highlighted as high (positive values) and low (negative values) anomaly years.

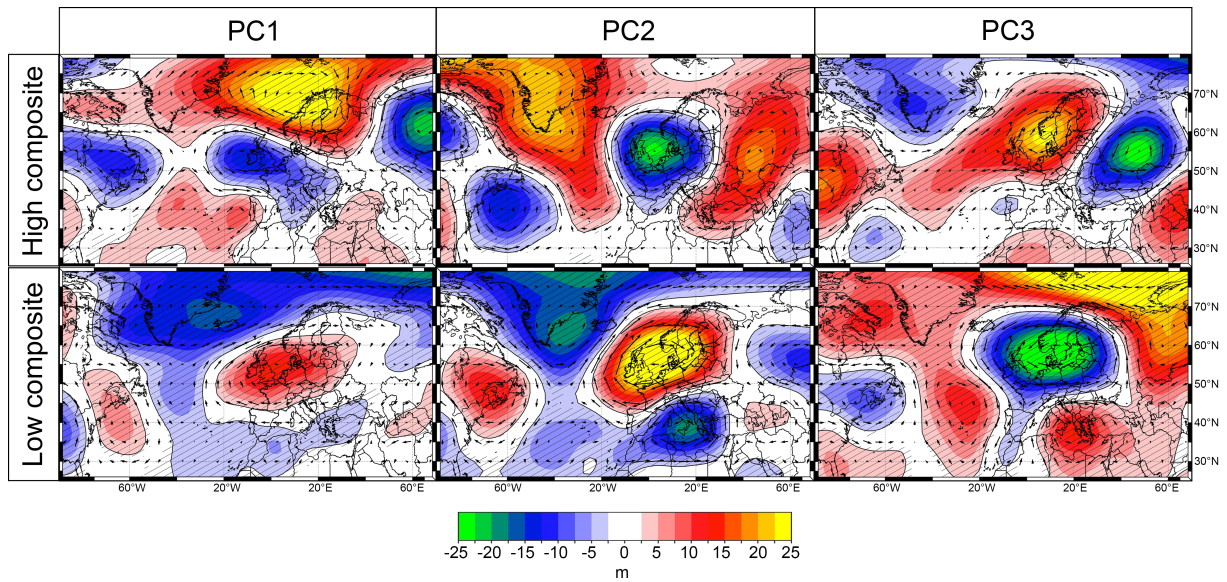


Figure 10. Composite maps of summer (June–August) Geopotential height at 500 mb (HGT500) anomaly relative to 1971–2000 for the first three PCs. High and low composites maps are shown, representing years with (positive and negative) values more extreme than one standard deviation in the corresponding PC time series.

Appendix A

A1

Streamflow regimes shown in Fig. 1 are calculated following the regime classification of Gottschalk et al. (1979), which consists of five main classes: Mountain, Inland, Transition, Baltic, and Atlantic regime. The classification is based on when high and low monthly streamflow typically occur during the year. Exact periods of low and high flow occurrences for each class are not provided in Gottschalk et al. (1979). Thus, we had to make choices regarding which months to be included for the definition of each class. Specifically, we calculated the 1959–2018 average mean streamflow for each month, and classified the stations as follows:

- Mountain regime is characterised by the two months of lowest flow occurring in winter or early spring due to snow accumulation, and the three months of highest flow occurring in spring or early summer due to snow melt. Because the snow melt season typically occur later with increasing altitude or latitude, a somewhat generous period for snow melt was applied. Mountain regime was assigned to stations with the two lowest monthly flow in January–April and three highest monthly flow in March–August. November and December were not included in the low flow season because none of the streamflow stations had the minimum or second minimum flow in these months. Whereas most Mountain regimes in this study had a distinct maximum flow in May or June, three of them had a later and less distinct peak in July. The later high flow peak is explained by the contribution of melt water from glaciers, which cover more than 30 % of the catchment of these three stations.
- Inland regime also have low flow during winter or early spring and high flow during snow melt, however, the second or third highest monthly flow occur during rainfall in autumn. Thus, the same months as for Mountain regime were used to define low flow period and snow melt period, whereas the autumn period was defined as September–November.
- Atlantic regimes have the highest monthly flow in autumn or winter due to rainfall, and the two months with lowest flow during summer or autumn due to high evapotranspiration and/or low precipitation. Atlantic regime was assigned to stations with the highest monthly flow in September–February and the two lowest monthly flows in June–October.
- Baltic regime have the same definition of the low flow period as Atlantic regime. However, either the second or third highest monthly flow occurs in September–February, whereas the highest flow occur during the snow melt period, here defined as March–May.
- Transition regime was assigned to stations that was not assigned to any of the other regimes, and is an intermediate regime between Inland and Baltic regime.

A2

The groundwater regime classification in Fig. 2 is based on the classification of groundwater fluctuation patterns by Kirkhusmo (1988) who divides groundwater fluctuation patterns into three idealised regions, with the possibility of a time shifted version

- of each fluctuation pattern. Region I represents groundwater levels reaching their maximum in late winter or early spring and their minimum in late summer (similar to Atlantic streamflow regime), Region II consists of groundwater levels with two annual maxima and two annual minima (similar to Transition streamflow regime), and Region III represent groundwater levels with a minimum just before the snowmelt, and a maximum after the snowmelt (similar to Mountain streamflow regime). In
- 5 this study, we calculated the 1989–2018 average-mean groundwater level for each month and defined the classes as follows:
- If the three months with highest groundwater level occur in October–April or in January–May and the three months with lowest groundwater level occur in June–December, the groundwater station was classified as belonging to Region I.
 - If the three months with highest groundwater level occur in April–July and all the three months with lowest groundwater level occur in December–May, the station was classified as Region III.

10

 - If instead of during April–July, the three months with highest groundwater level occur in May–November, and the three months with lowest groundwater level still occur in December–May, we assumed a time-lag effect and the station was classified as Region III delayed.
 - If neither of the above, and the groundwater level have two minima and two maxima during the year, the groundwater station was classified as Region II.

15

 - For the remaining three stations, the three months with highest groundwater level occurred in April–July and the three months with lowest groundwater level occurred in October–January, and these stations were classified as Region I delayed.

A3

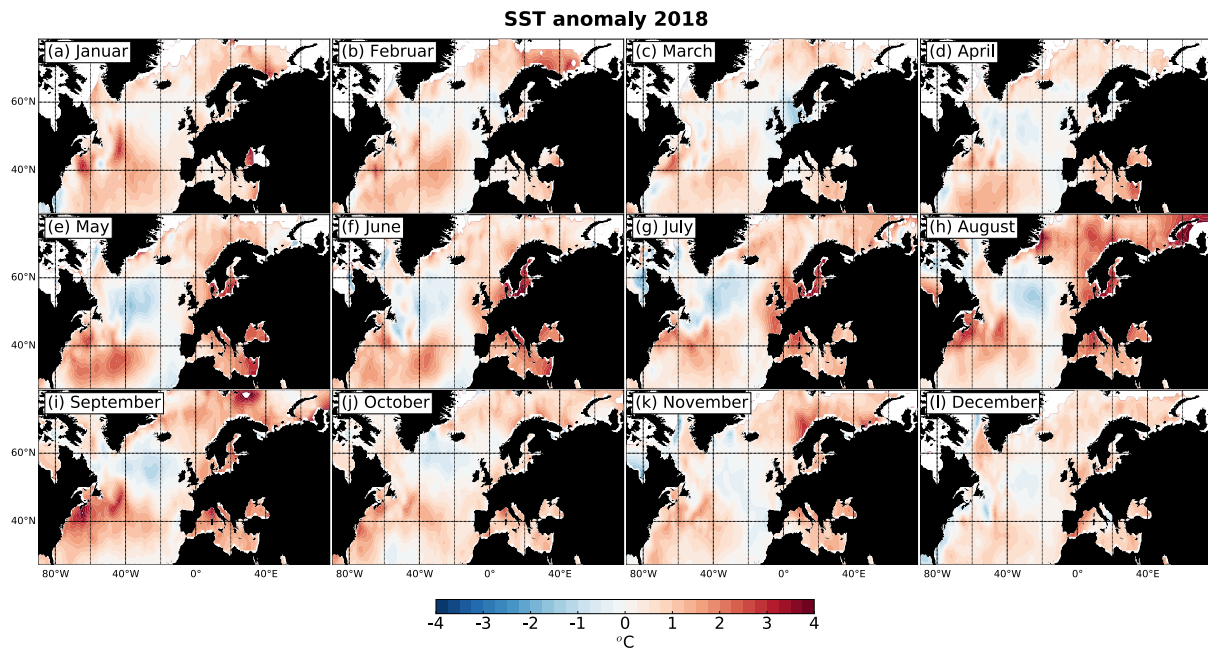


Figure A1. Monthly Sea Surface Temperature (SST) anomalies throughout 2018 relative to the reference period ~~+1981-2000~~ 1971-2000.

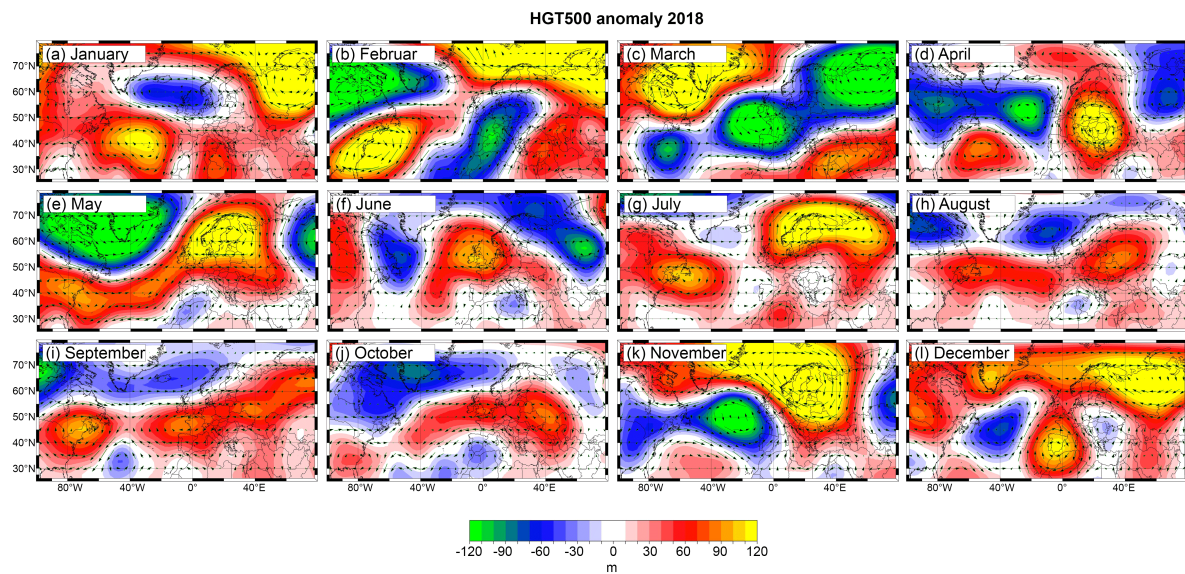


Figure A2. Monthly geopotential height at 500 mb (HGT500) anomalies throughout 2018 relative to the reference period 1971–2000.

HGT500 subdomain standard deviation

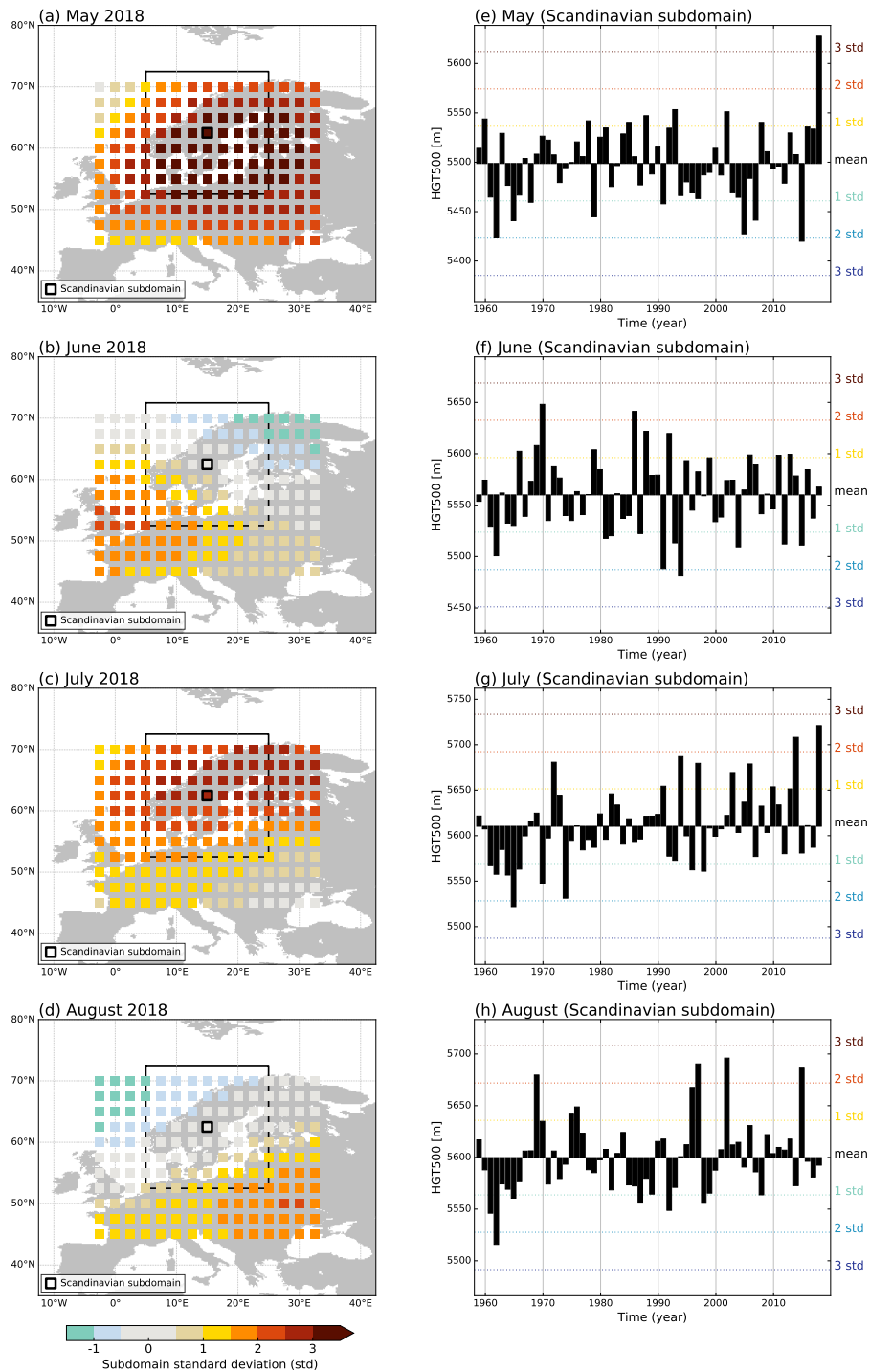


Figure A3. Left panel: Geopotential height at 500 mb (HGT500) shown as standard deviation (std) of (a) May, (b) June, (c) July and (d) August 2018 based on the 60-year period (1959–2018) for subdomains of 20° lon/lat throughout Europe, shifted 2.5° at a time. The coloured squares are the center points of each subdomain. This is illustrated for one subdomain over Scandinavia, with a large and a small square marking the subdomain's border and centerpoint, respectively. Right panel: HGT500 1959–2018 time series of (e) May, (f) June, (g) July and (h) August for the Scandinavian subdomain. Note the different ranges of the y-axes.

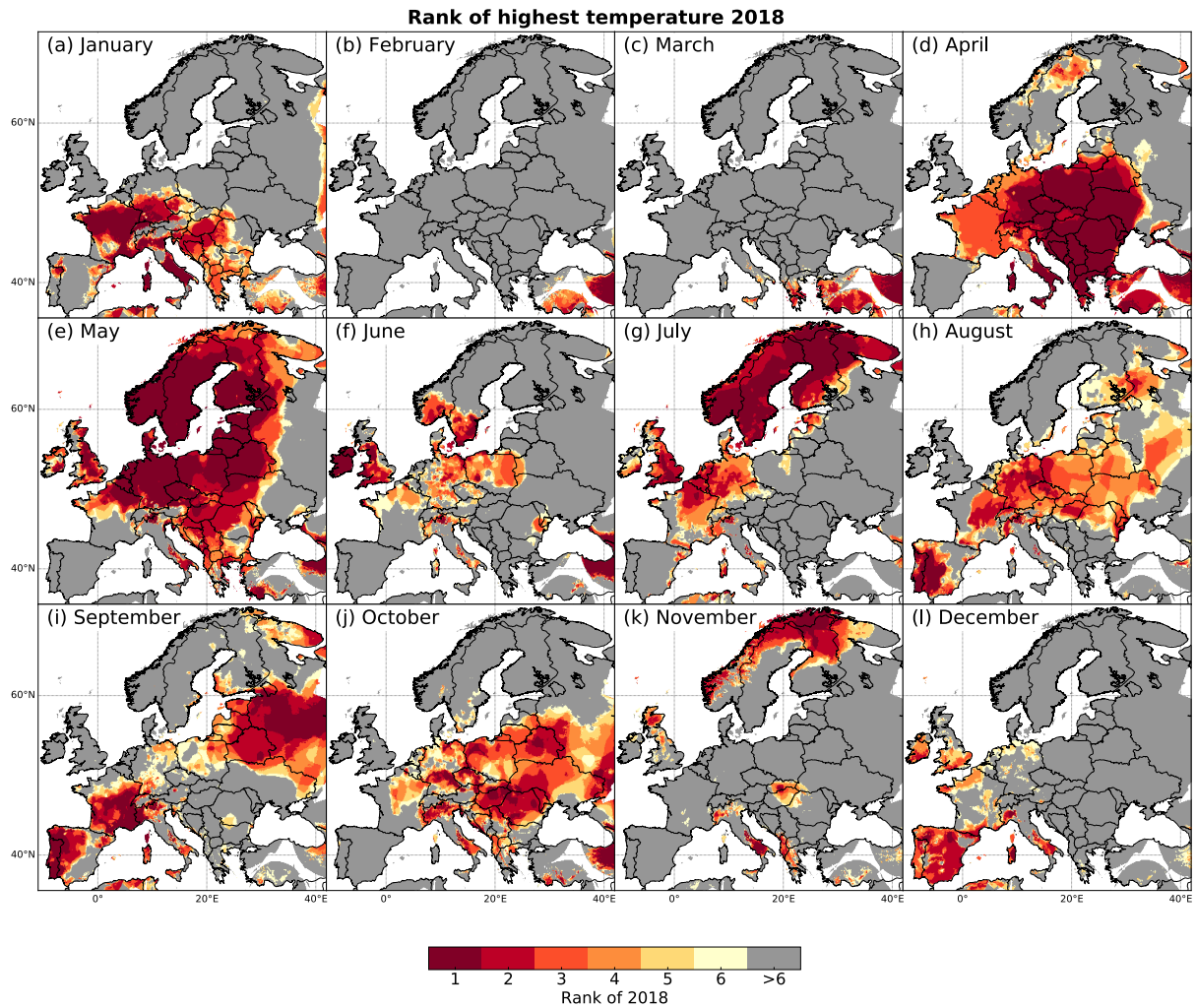


Figure A4. Top-six ranking of 2018 monthly highest temperature (monthly mean of daily maximum temperature) relative to the period 1959–2018.

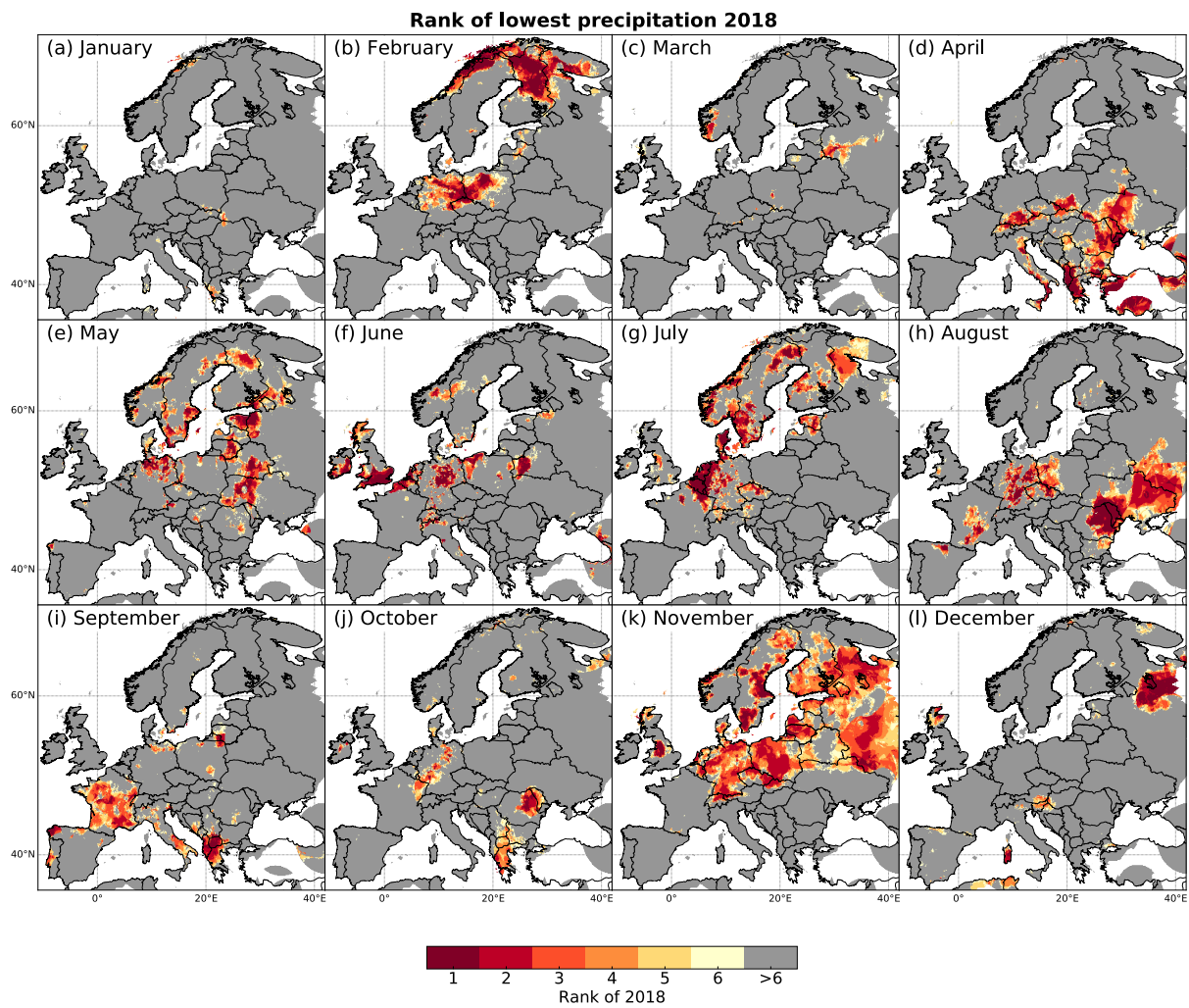


Figure A5. Top-six ranking of 2018 monthly lowest precipitation relative to the period 1959–2018.

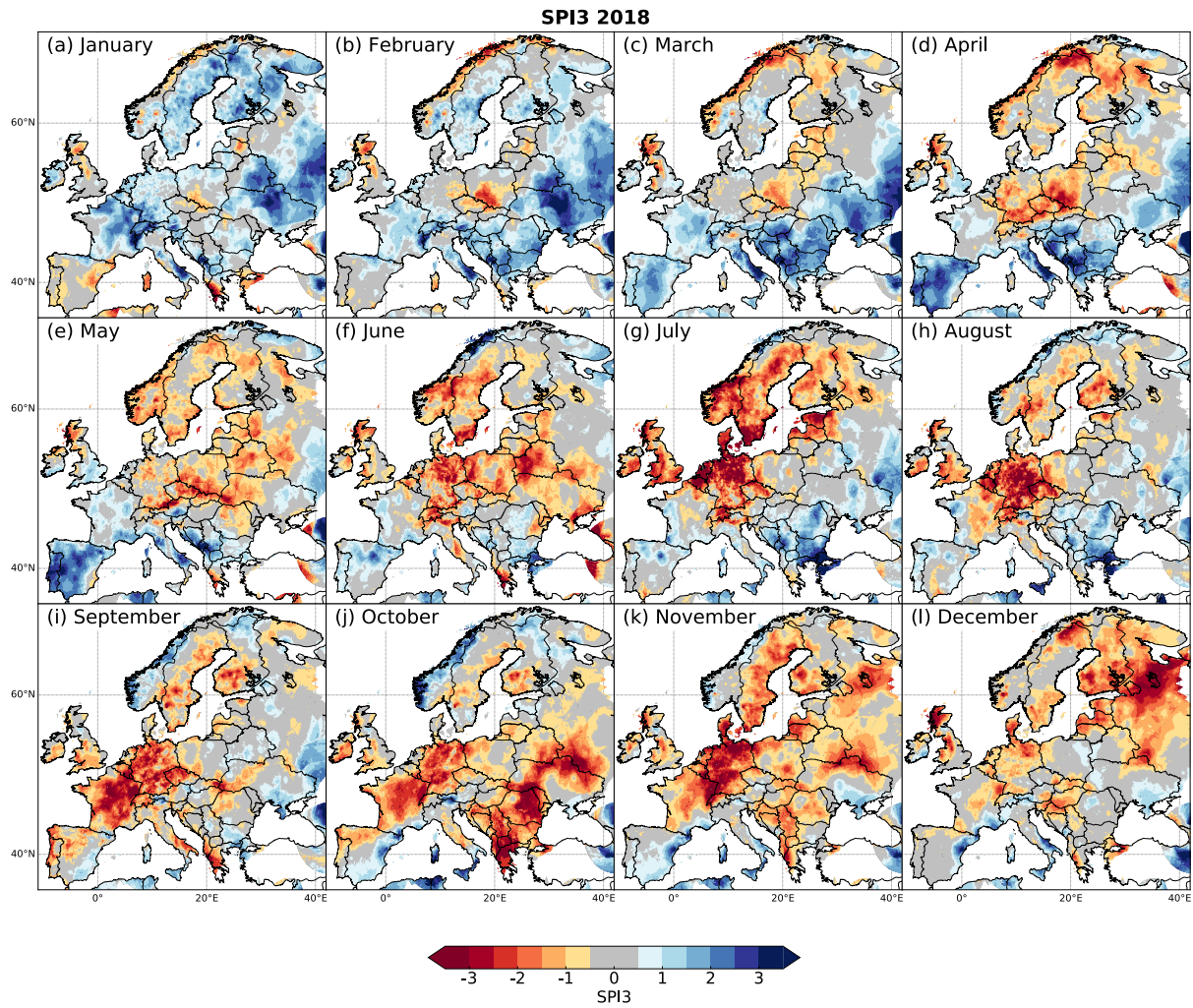


Figure A6. Monthly meteorological drought indexed by SPI3 throughout 2018 relative to the reference period 1971–2000.

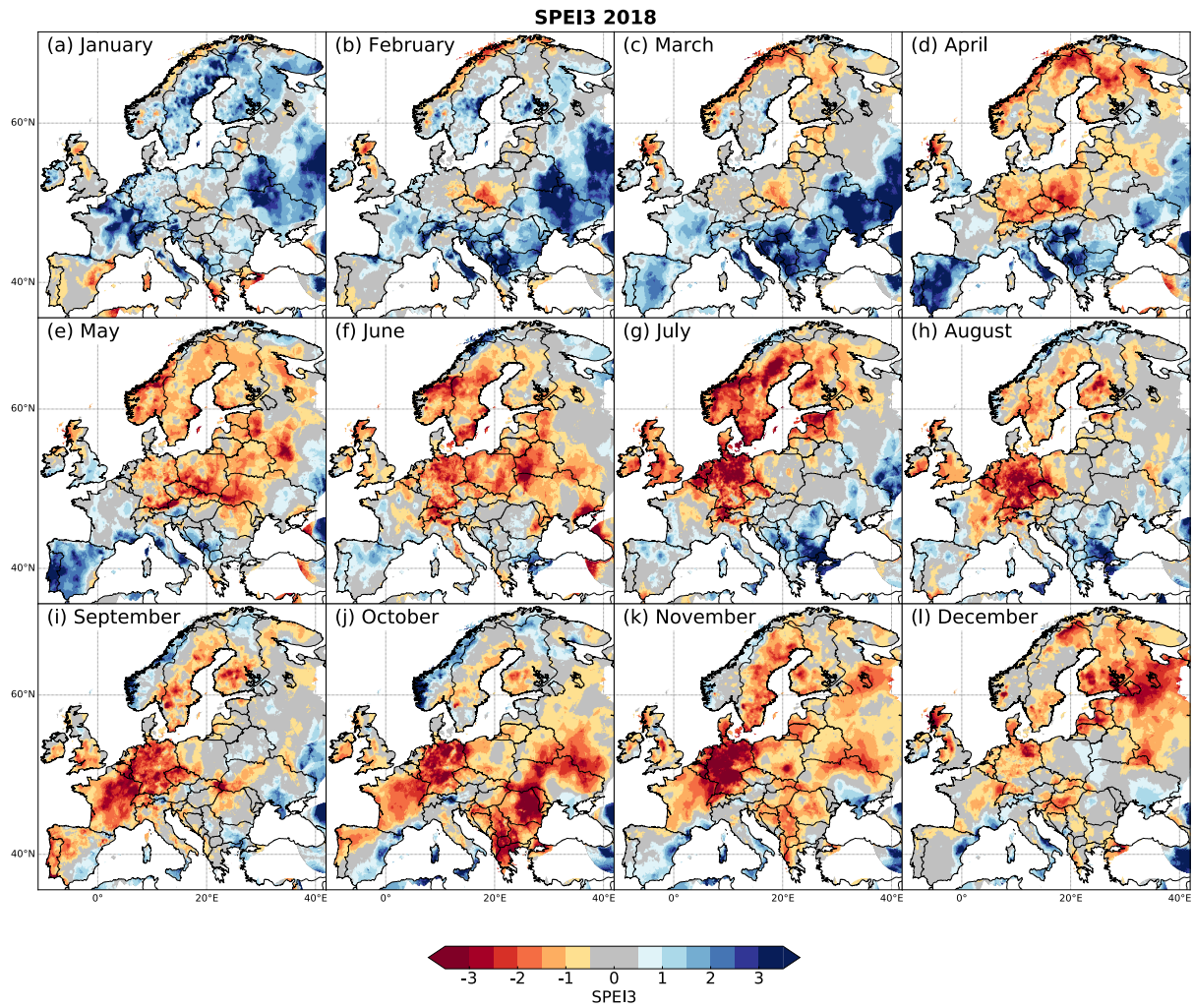


Figure A7. Monthly meteorological drought indexed by SPEI3 throughout 2018 relative to the reference period 1971–2000.

Rank of lowest streamflow 2018

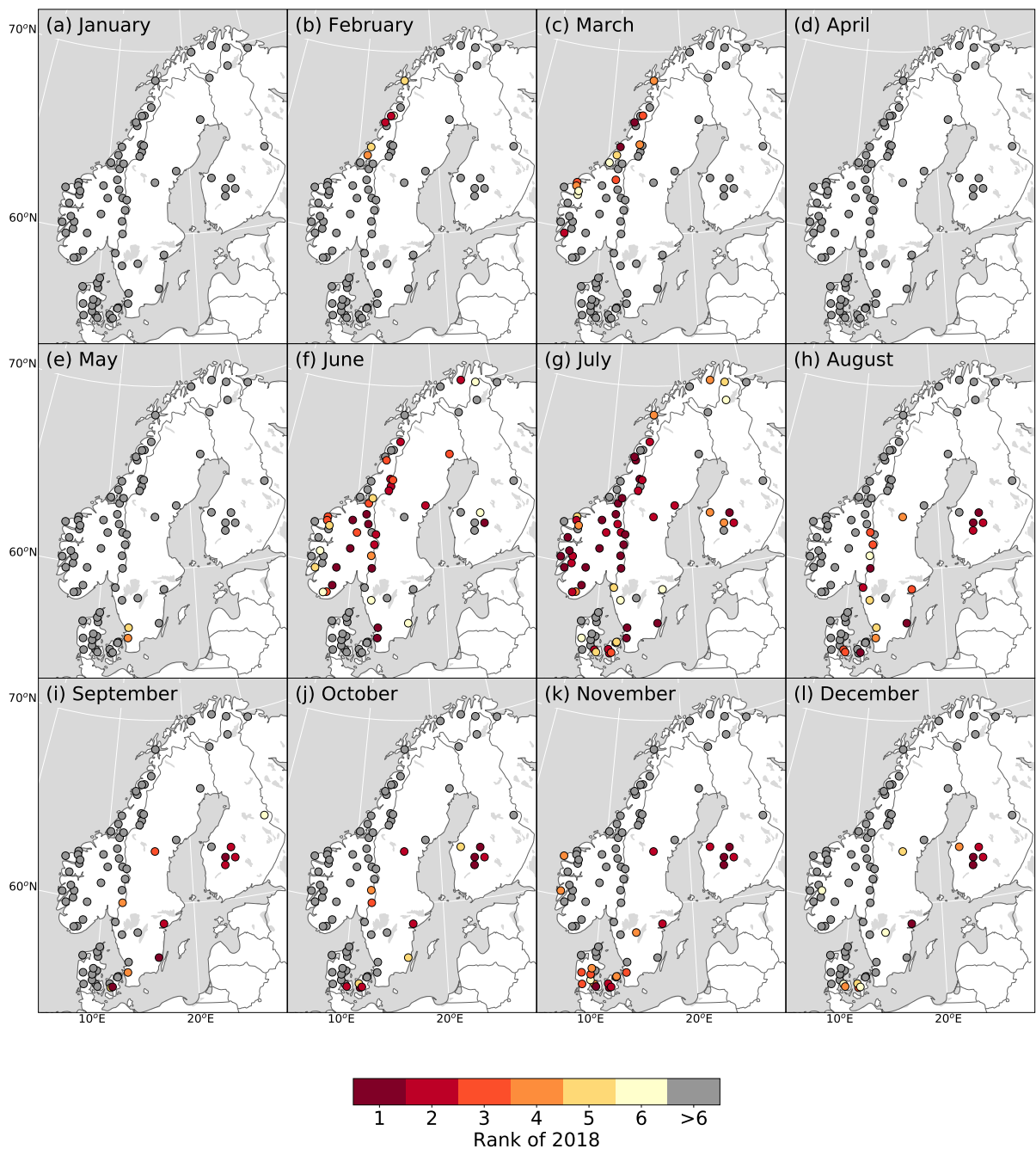


Figure A8. Top-six ranking of 2018 monthly lowest streamflow relative to the period 1959–2018.

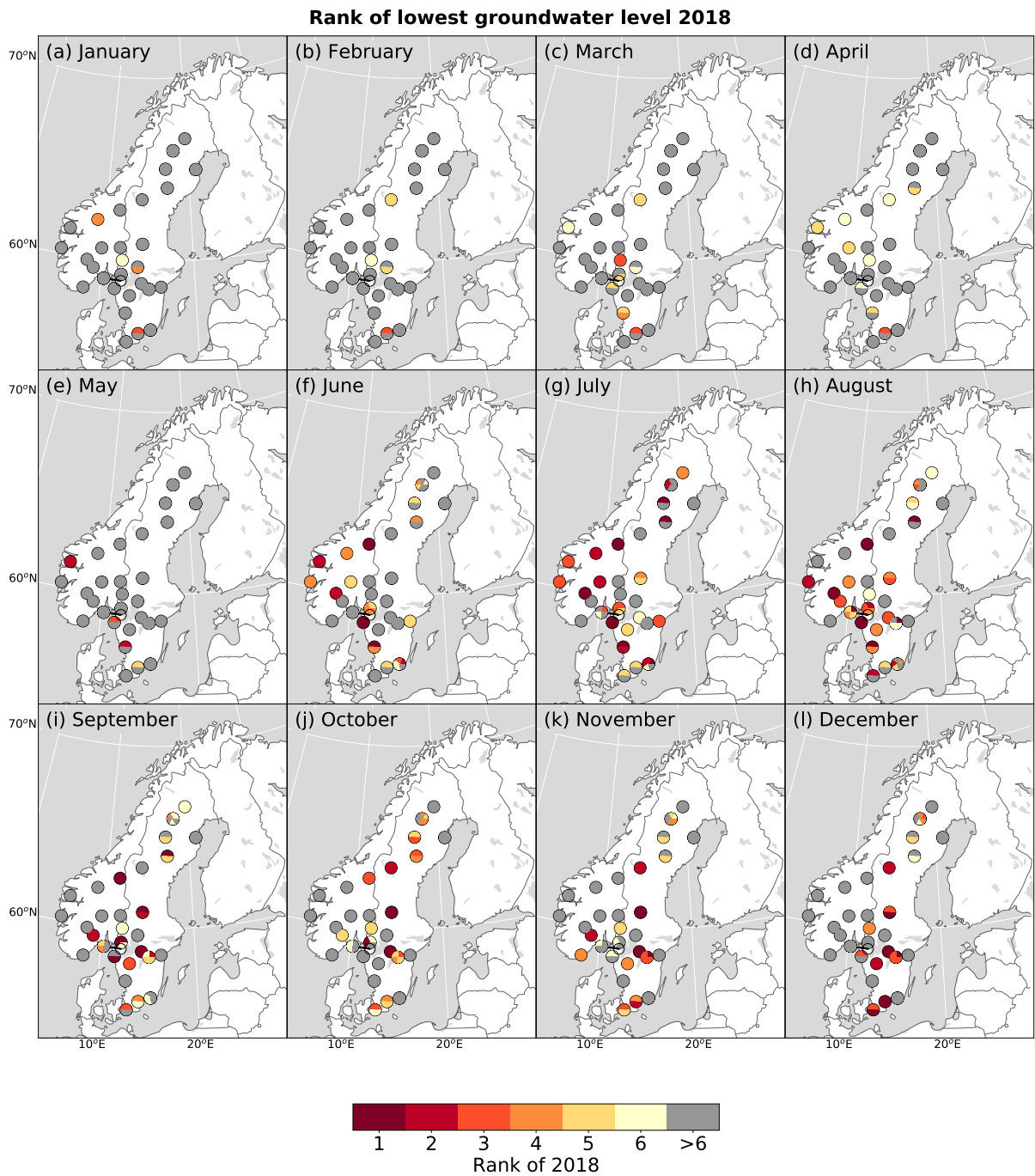


Figure A9. Top-six ranking of 2018 monthly lowest groundwater level relative to the period 1989–2018.